*ICES Journal of Marine Science*, 2026, Vol. 83, Issue 5, fsag082
https://doi.org/10.1093/icesjms/fsag082
**Original Article**

# Environmental DNA metabarcoding captures plankton diversity in the southern North Sea

**Ilias Semmouri [1,*], Michiel De Cooman [1], Enora Geslain [2,3], Filip a.m. Volckaert [2], Colin R. Janssen [1], Jana Asselman [1]**

[1]Blue Growth Research Lab, Ghent University, Bluebridge, Wetenschapspark 1, B-8400 Ostend, Belgium
[2]Laboratory of Biodiversity and Evolutionary Genomics, KU Leuven, B-3000 Leuven, Belgium
[3]Genomics Core of Leuven, UZ - KU Leuven, B-3000 Leuven, Belgium
*Corresponding author. Present address: Ghent University, Blue Growth Research Lab, Campus Coupure, Building F – 2nd Floor, Coupure Links 653 – B-9000 Ghent – Belgium. Email: Ilias.Semmouri@UGent.be

## Abstract

**DNA metabarcoding is increasingly used to monitor marine plankton communities. Here, we investigated the taxonomic diversity and community structure of eukaryotic plankton, including well-studied phytoplankton and mesozooplankton, as well as lesser-known taxa in the Belgian part of the North Sea. We used an integrative morphological and molecular approach, combining environmental DNA (eDNA) metabarcoding with imaging of plankton samples, collected using plankton nets and analyzed via either FlowCAM or ZooScan. Water samples were collected over one year and analyzed based on a 650 bp fragment of the 18S rRNA V4–V5 region using Oxford Nanopore sequencing. Across 77 samples, we examined community composition and diversity metrics at the phylum level and compared molecular results (after normalization of read numbers) with morphological assessments. Diversity indices were positively correlated with nutrient concentrations and turbidity, but negatively with water temperature. No correlation was found between microalgal cell density and taxon richness, although cell density correlated negatively with diversity indices incorporating evenness. Metabarcoding identified 25 phyla not detected morphologically, including four fungal phyla, picozoans, and loukozoans. Significant correlations were observed between eDNA-derived abundances (based on both rarefied read counts and the eDNA index) and morphological densities for the dominant phyla (Arthropoda and Myzozoa), whereas no such relationships were found for less abundant taxa. However, discrepancies remained between relative abundances derived from morphology and DNA reads, reflecting differences in taxonomic resolution and detection biases. Overall, eDNA metabarcoding provided broader taxonomic coverage, while morphological methods offered finer taxonomic resolution of a limited selection of taxa.**

**Keywords** 18S rRNA barcode, biomonitoring, MinION, nanopore sequencing, phytoplankton, zooplankton

## Introduction

The adoption of the 2020 Strategic Plan for Biodiversity and its 20 Aichi Targets at the tenth Conference of the Parties to the Convention on Biological Diversity (CBD) in Nagoya in 2010 represented a pivotal moment in global biodiversity conservation (Brooks et al. 2015). Considering unprecedented changes to the rate of biodiversity loss due to anthropogenic disturbance and the importance of long-term spatial and temporal monitoring of marine communities, it was considered essential to develop rapid but solid biodiversity survey tools to monitor changes in species richness to help inform conservation and management strategies (Kelly et al. 2014, Ratnarajah et al. 2023). The UN has declared 2021–2030 the Decade of Ocean Science to advance Sustainable Development Goal (SDG) 14–conservation and sustainable use of marine resources—emphasizing the need for ocean research to deliver clear societal benefits (https://en.unesco.org/ocean-decade). However, because the Aichi Targets were established relatively recently, there remains a significant gap in investment for monitoring biodiversity toward achieving these goals (Brooks et al. 2015). Furthermore, accurately monitoring subtle changes in community dynamics requires high-frequency sampling. Traditional net-based and microscopy-based analyses are resource-intensive and require specialized expertise, which often constrains sampling frequency. Thus, detecting the presence of multiple species through DNA extracted from environmental samples (known as “environmental DNA” or “eDNA”) using high-throughput sequencing has been put forward as a rapid and time efficient approach for surveying species richness in natural communities (Creer et al. 2016, Deiner et al. 2017). Environmental DNA are traces of DNA which can be retrieved from e.g. mucus, shed (skin) cells, feces, gametes and organelles, degrading tissue, and whole organisms, and are typically sampled from sea- and freshwater, soil, air, sediment, ice or permafrost (Deiner et al. 2017).

**Received:** 11 February 2026. **Revised:** 20 April 2026. **Accepted:** 28 April 2026

Environmental DNA metabarcoding can potentially enhance and address limitations of conventional methods by targeting a wider range of species, sampling greater diversity, and improving the resolution of taxonomic identifications. It is therefore regarded to be a cost- and time efficient method, being less laborious to traditional methods, and it generally causes less disturbance to the marine environment compared to morphological sampling (Takasu et al. 2019, Ames et al. 2021, Miya 2022). Also, recent advances in autonomous monitoring and marine robotics for eDNA sampling further propel this technique as high throughput monitoring alternative. Yet, the technique comes with several limitations: metabarcoding results strongly rely on the sensitivity and taxonomic coverage of the genetic markers (Zhang et al. 2018, Li et al. 2020). DNA metabarcoding is subject to observation bias associated with PCR and sequencing, and—additionally—variation in gene copy number across taxa can introduce biases in metabarcoding-based abundance estimates, further complicating quantitative interpretations (e.g. Barnes and Turner 2016, Shaffer et al. 2025). The completeness of reference sequence databases varies widely as well across taxonomic groups and ecosystems, and remains particularly limited for species-rich but understudied taxa and regions (e.g. Bucklin et al. 2021, Keck et al. 2023, Leray and Knowlton 2015 ). For example, Schoch et al. (2020) compared the number of formal species listed in the NCBI Taxonomy database with those recorded in various catalogues. Their analysis revealed that, in 2019, 83% of described invertebrate taxa were absent from the NCBI Taxonomy. Similarly, Weigand et al. (2019) reported significant disparities in the representation of taxonomic groups used for ecological monitoring of aquatic environments in Europe within reference databases. Specifically, groups such as fish and freshwater vascular plants were substantially better represented compared to others, including ascidians, freshwater diatoms and marine mollusks.

Plankton constitutes an important link in the pelagic food web and contributes to the biological pump as sources or sinks of $CO_2$ and other greenhouse gasses through the formation of marine snow (Kiørboe 2001). Moreover, as planktonic assemblages rapidly respond to environmental variation (i.e. by changes in community structure, biomass and trophic linkages), they are applicable as bio-indicators of ecosystem change (Ferdous and Muktadir 2009, Chiba et al. 2018). For example, the Convention for the Protection of the Marine Environment of the North-East Atlantic (OSPAR convention) currently uses plankton-based indicators to evaluate the Good Environmental Status (GES) of pelagic habitats across the North-East Atlantic region (Rombouts et al. 2019).

Despite their ecological importance, spatiotemporal variations in plankton assemblage composition remain incompletely characterized for many taxa and regions, partly due to challenges in taxonomic identification and the time required for morphological analyses (e.g. Djurhuus et al. 2018, Robinson et al. 2021, Peng et al. 2024). Furthermore, sampling plankton communities comprehensively presents technical challenges due to their immense size range, spanning more than six orders of magnitude—from less than a micrometer to several meters. Here, eDNA metabarcoding of plankton communities offers a promising solution to some of these limitations. However, the application of this method on planktonic taxa remains limited. Most studies (63% of recovered studies, n = 407) focus on charismatic aquatic taxa such as teleost fish, mammals, and amphibians, as highlighted by the systematic literature review on aquatic eDNA by Takahashi et al. (2023). In comparison, cnidarians and arthropods accounted for approximately 10% of the collected studies, while other planktonic taxa were examined in less than 1% of these studies. Nevertheless, a growing body of research has adopted eDNA metabarcoding approaches to profile plankton assemblages (e.g. Hendricks et al. 2023, Doğan et al. 2025, Liang et al. 2025).

In addition to molecular approaches, plankton research is increasingly exploring automated image-based methods for rapid and high-throughput community assessment. Techniques such as FlowCam and ZooScan enable semi-automated identification based on organism morphology (e.g. Álvarez et al. 2011, Naito et al. 2019, Grandremy et al. 2023). However, graphical identification methods are limited by image resolution and orientation, which can hinder accurate taxonomic classification, particularly for small, morphologically similar, or partially obscured organisms. In addition, they often require extensive training datasets or expert validation, introducing potential biases and reducing consistency across studies.

The Southern Bight of the North Sea encompasses the relatively shallow (maximum depth of 40 m) and well-mixed Belgian part of the North Sea (BPNS; encompassing both terrestrial waters and exclusive economic zone). The area is subject to a wide array of anthropogenic pressures, including sand extraction, anchorage zones, intensive fisheries including beam trawling, chemical pollution, submarine cables, and the introduction of invasive and potentially harmful species via ballast water (Lescrauwaet et al. 2013). Furthermore, recent observations have identified the North Sea as the fastest-warming region within the entire Atlantic Ocean over the past four decades, with sea surface temperatures increasing at a rate of $0.39 \pm 0.06^{\circ}C$ per decade (Kessler, Goris and Lauvset 2022). These factors collectively underscore the BPNS as a highly pertinent case study, offering valuable insights applicable to coastal ecosystems worldwide. Apart from some recent meso- and macrozooplankton (Vansteenbrugge et al. 2015a, Van Ginderdeuren et al. 2014, Semmouri et al. 2020, Mortelmans et al. 2021, 2023, 2024a) and phytoplankton studies (Amadei Martínez, Mortelmans and Dillen 2020; Nohe et al. 2018, Mortelmans et al. 2024, Liu et al. 2025), information on pelagic planktonic life from the southern North Sea is currently limited. Nevertheless, environmental changes have been shown to significantly influence the plankton community in this region. For example, a significant decrease (up to two orders of magnitude) over the last decade was observed in the abundance of several species of the dominant group of mesozooplankton of the BPNS, i.e. calanoid copepods, with local (temporary) absences coinciding with intensive heat waves in summer (Semmouri et al. 2023). More recently, Mortelmans et al. (2024) suggested that the absence of zooplankton predators in summer-autumn, together with the availability of nutrients, allowed bloom formation of the diatom *Bellerochea* sp., in a season otherwise characterized by relatively low phytoplanktonic activity. Together, these studies suggest that the plankton communities in the BPNS are changing, and therefore, require further study to document these changes.

To improve plankton monitoring, it is essential to identify which taxa are detected or overlooked by different methodological approaches. In this context, we applied an eDNA metabarcoding approach targeting the 18S rRNA gene region to investigate spa-

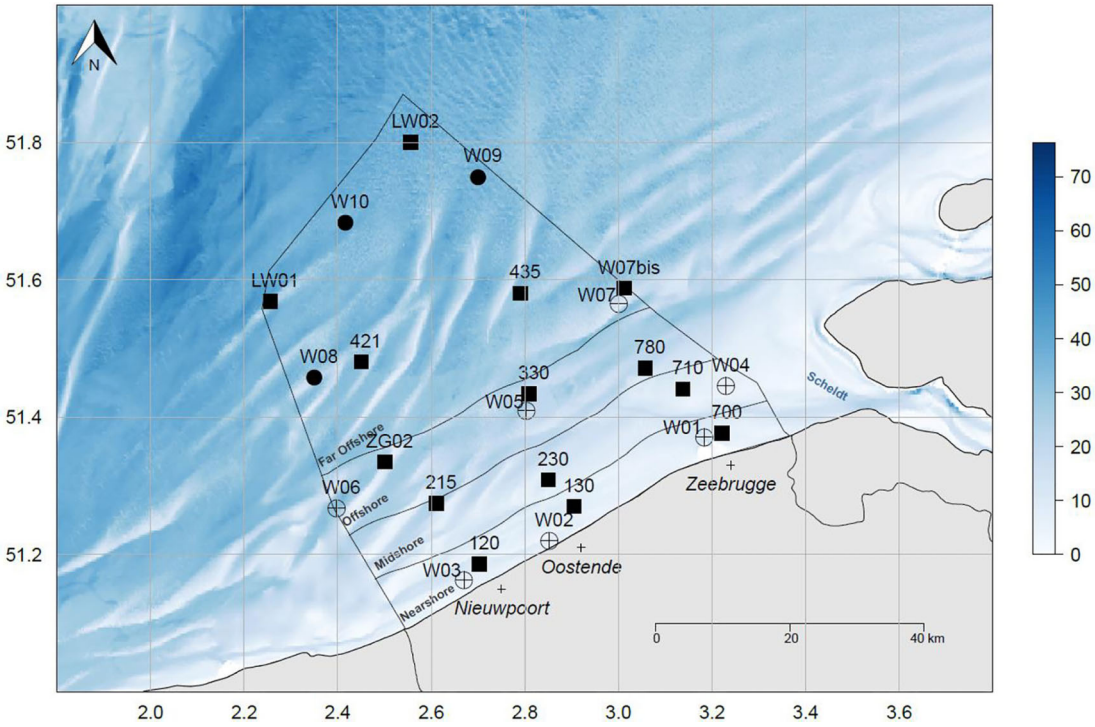


**Figure 1.** Map illustrating study sites (stations) of this study in the Belgian Part of the North Sea (BPNS) and stations, as indicated by the black squares. Nine stations were visited monthly: 130, 780, 330, 230, 710, 215, ZG02, 120 and 700, while the other 8 offshore stations were only visited two times. Station names (i.e. sampling locations) are indicated above the labels. The zones nearshore, midshore, offshore and far offshore are indicated on the map. Bathymetry in meter (m) is reported in the associated legend. Crosses indicate major coastal cities. Exact sampling coordinates and dates are provided in Supplementary Table S1. Modified from Mortelmans et al. (2019) with permission from the authors.

tiotemporal patterns of the eukaryotic pelagic community in the BPNS over the course of one year. A ~650 bp fragment encompassing the V4–V5 region was sequenced using the MinION™ nanopore platform (Oxford Nanopore Technologies). Although this marker can achieve species-level resolution in some groups, its taxonomic resolution varies across lineages (e.g. Pawlowski et al. 2012, Hadziavdic et al. 2014). Therefore, analyses were conducted at the phylum level to ensure robustness and comparability.

The performance of this metabarcoding approach was evaluated alongside automated image-based methods, specifically ZooScan for mesozooplankton and FlowCam for phytoplankton, which offer time-efficient alternatives to traditional microscopy. However, all these approaches are not directly comparable due to inherent differences in sampling design and detection capacity. eDNA samples were collected at a fixed shallow depth (3 m), whereas the WP2 and Apstein net samples integrate across the water column. Moreover, net sampling is size-selective, while eDNA can capture a broader range of taxa, including smaller organisms below mesh size and larger, rare species that may be missed. Although such differences partly reflect the strengths of eDNA, they also highlight that these methods do not represent like-for-like comparisons.

This study addresses the following questions: (1) which taxa can be detected using eDNA from filtered water samples; (2) whether spatiotemporal patterns in plankton diversity and community composition can be identified; (3) to what extent eDNA reflects plankton presence and/or abundance; and (4) which environmental variables are associated with observed community patterns. In doing so, this work contributes to identifying understudied plankton taxa relevant to coastal ecosystem monitoring.

# Material and methods

## Sampling campaigns and measurements of environmental variables

Water samples were taken with research vessel (RV) *Simon Stevin* on nine one-day sampling missions in 2022 and 2023 (starting on 17$^{th}$ of August 2022, ending on 21$^{st}$ of September 2023) at nine sampling locations in the Belgian part of the North Sea (BPNS) and eight additional offshore stations in September and October 2022 (Fig. 1). Due to bad weather conditions or technical issues, no samples were collected between February and May 2023. Supplementary Table S1 provides precise sampling dates and GPS coordinates. Sampling was repeated twice for two samples (station 130, August 2022; station ZG02, December 2022) to control for sample variability. In total, 89 seawater samples (i.e. 22 nearshore, 22 midshore and 45 (far) offshore samples) were taken throughout the sampling period.

Water samples were collected by means of a CTD (Conductivity-Temperature-Density) carousel, equipped with six teflon-coated Niskin bottles (Supplementary Fig. S1), of which one was filled with seawater at a depth of three meters. The Niskin bottle was thoroughly rinsed with tap water between sampling. The water samples were filtered on board of the RV, using Supor 200 mem-

brane disc filters (PALL 60301, 0.2 μm pore size, 47 mm diameter), which were afterwards folded in eight and stored in labelled 2 mL Eppendorf tubes in the freezer (-16°C) of the RV. Three replicates were taken per station and 600 mL water was filtered per replicate. The limited sample volume may have constrained detection sensitivity and the completeness of plankton community characterisation. Due to elevated concentrations of suspended particles in the water column in nearshore locations, no larger volumes could be filtrated. In order to avoid contamination between sampling stations, the filtration cups were thoroughly cleaned in between sampling with tap water and subsequently with 70% ethanol. At each sampling campaign, two blank samples (using 600 mL of tap water) were collected in between sampling stations to assess for cross-contamination between sampling stations, following the same procedure as described above. Immediately after the sampling campaign, the stored filters were taken to the laboratory in Ghent and stored at -80°C untill further processing. Additional controls were performed in the lab with deionized water following the same procedure.

Additionally, phytoplankton samples were obtained by filtering 50 L of surface seawater using a closing Apstein plankton net (10 cm mouth diameter, 55 $\mu$m mesh size). Phytoplankton densities were then quantified and identified with the Flow Cytometer And Microscope (FlowCAM®) and associated image-based classification, following the protocol of Lagaisse (2024). Briefly, 50 L of surface seawater were collected, filtered, and analyzed with a FlowCam VS-4 benchtop system (Fluid Imaging Technologies, Yarmouth, Maine, USA) to classify particles into distinct taxonomic groups. Additional methodological details are provided in the supplemental methods and in Amadei Martínez et al. (2020).

Finally, at each sampling location, mesozooplankton samples were collected using a WP2 net (57 cm in diameter; 200 μm mesh size) that was hauled vertically from bottom to surface at each station. To ensure preservation, formaldehyde was added to the collected samples, containing seawater and plankton, until a 6% final concentration was reached. The complete sampling protocol is described in (Mortelmans et al. 2019). A fraction of the sampled volume of all these samples have been digitized by the ZooScan plankton imaging device (HYDROPTIC, France), producing high-resolution digital scans of preserved zooplankton, as described in Mortelmans et al. (2019). The ZooProcess software (v8.04) consequently processed these scans and identified the zooplankton to the lowest resolution possible.

At each sampling station, we conducted CTD (conductivity, temperature, and depth) profiling using a Seabird 25plusV2 CTD system (Flanders Marine Institute 2024a). Additionally, the following environmental parameters were measured at a 3-meter depth in the water column: salinity (ppt), optical backscatter (OBS; a measure for water column turbidity, expressed in Nephelometric Turbidity Units, NTU), and fluorescence (an indirect estimate of phytoplankton biomass, particularly the concentration of chlorophyll *a*), expressed in $mg.m^{-3}$. An additional water sample was obtained at each sampling site using a second Niskin bottle at a 3-meter depth and later analyzed for nutrient concentrations, as part of the Flemish contribution to the LifeWatch ESFRI by Flanders Marine Institute (Flanders Marine Institute 2024b). For nutrient analysis, 200 mL of seawater was filtered using cellulose-acetate filters to remove residual water, and the concentrations of nitrate ($NO_3^-$), nitrite ($NO_2^-$), ammonium ($NH_4^+$), phosphate ($PO_4^{3-}$), and silicate ($SiO_4^{4-}$) were determined using a QuAAtro39 Continuous Segmented Flow Analyzer (SEAL Analytical GmbH, Norderstedt, Germany), as described in Mortelmans et al. (2019).

## DNA extraction and amplification

Environmental DNA (eDNA) of all samples was extracted using the QIAGEN DNeasy® Blood & Tissue Kit according to the manufacturer's instructions with some minor modifications. Briefly, the filters containing eDNA were cut in half and placed in 2 mL Eppendorf tubes, after which 165 μL ATL buffer was added twice to each tube, separated by a 30 min incubation period at 56°C. Afterwards, 20 μL Proteinase K was added and the tubes were incubated for 2 h at 56°C in a VWR Incubating Mini Shaker. The dislodged eDNA (supernatant) was then transferred into a new 2 mL Eppendorf tube, after which the tubes were centrifuged to create a pellet. Once again, the supernatant was transferred to a new tube and mixed with 320 μL AL buffer and 320 μL ethanol (96%-100% for molecular biology purposed, Sigma-Aldrich, CAS-No: 64–17-5). This solution was then sent through the filter of a DNeasy spin column via centrifugation. The filters of the spin column were washed using 500 μL AW1 and 500 μL AW2 buffer, respectively. Finally, 30 μL AE buffer was sent through the filter to retrieve the DNA twice, in order to have two elution series. The quality of the DNA extractions was investigated using the Nanodrop 2000 Spectrophotometer (Thermo Scientific) through evaluation of the 260/280 and 260/230 ratios.

After extraction, samples of satisfying quality (77/89) were amplified using an adapted version of the primer pair F-566 and R-1200 of the 18S ribosomal DNA gene (sequences (5'–3') CAG CAG CCG CGG TAA TTC C and CCC GTG TTG AGT CAA ATT AAG C, respectively), selected for their wide taxonomic range (Hadziavdic et al. 2014). Theoretical coverage reached 80% and empirical data showed amplification for 71% of all eukaryotic phyla (Hadziavdic et al. 2014). To multiplex all samples in an additional PCR round, an ONT adapted 18S rRNA forward/reverse primer pair was used [sequences (5'-3') TTT CTG TTG GTG CTG ATA TTG C CAG CAG CCG CGG TAA TTC C and ACT TGC CTG TCG CTC TAT CTT C CCC GTG TTG AGT CAA ATT AAG C, respectively]. Amplifications were performed in volumes of 50 μL containing 25 μL Invitrogen Platinum Hot Start PCR 2X Master Mix, 1 μL of 20 μM forward and reverse primer stock solution and 0.5–5 μL template DNA (±100 ng). The solution was then diluted with DNase free water (NFW) until 50 μL. PCR amplification was carried out using the PCR thermocycler (Analytic Jena 846-x-070–280 Biometra TAdvanced Unit), which was set at 94°C for 2 min to activate DNA polymerase. The PCR reaction itself consisted of 35 cycles of denaturation at 94°C for 30 s, annealing at 55°C for 30 s and extension at 72°C for 1 min. For each amplification, 1.5% agarose gel electrophoresis was performed to evaluate if PCR was successful, with success being indicated by the presence of a band for each sample (2 μL/sample, stained with 1 μL ThermoFisher Scientific DNA gel loading dye per sample) around 500–700 base pair amplicons on the gel. Amplicon length was assessed by comparison with 6 $\mu$L of ThermoFisher Scientific GeneRuler 100 bp DNA Ladder in the first well.

In an additional PCR round, Oxford Nanopore barcode tag sequences were added to the amplicons from the second PCR round, enabling multiplexing, using the SQK-LSK110 protocol of Oxford Nanopore Technologies (2023). Amplifications were performed in

volumes of 50 μL containing 25 μL LongAmp Taq 2x master mix, 1 μL of PCR Barcode (Oxford Nanopore Kits, one of BC1-BC96, at 10 μM), 1 μL final PCR product and 23 μL DNase free water. After mixing by pipetting up-and-down and a brief centrifugation (short spin of 5–10 s, VWR Galaxy Minicentrifuge SN 0910 0713), PCR amplification was carried out using the PCR thermocycler, which was set at 95°C for 3 min for initial denaturation, followed by a PCR reaction consisting of 20 cycles of denaturation at 95°C for 15 s, annealing at 62°C for 15 s and extension at 65°C for 90 s, according to the barcoding PCR protocol of Oxford Nanopore Technologies (2023). The DNA quantity in the samples was determined using a QubitTM fluorometer (Version 2.0, InvitrogenTM, Thermo Fisher Scientific). Samples were stored at − 80°C until library preparation.

## Library preparation and DNA sequencing using the MinION platform

Library preparation and DNA sequencing were performed using the 1D PCR barcoding Expansion Pack 1–96 (EXP-PBC096) with the SQK-LSK114 kit (Oxford Nanopore Technologies 2023). All barcoded libraries were equimolarly pooled to obtain 1 μg eDNA in total in a 1.5 mL DNA LoBind Eppendorf tube. Library preparation was carried out according to the manufacturer's protocol with slight adaptations. Briefly, amplicons were end-repaired using 3 μL NEBNext Ultra II End-Repair/dA-tailing enzyme mix (E7546) at 20°C for 5 min and 65°C for 5 min, after which they were purified with 60 μL of resuspended CleanNGS beads. Next, adapter ligation was carried out with 25 μL of Ligation Buffer (LNB), 5 μL of Ligation Adapter (LA), and 10 μL of NEBNext Quick T4 DNA Ligase (New England Biolabs, USA), followed by another purification step using the magnetic beads. The washing step, using 250 μL of Short Fragment Buffer (SFB), was performed twice before the DNA was eluted by incubation in 15 μL of Elution Buffer (EB) for 10 min. Then, 12 μL of the amplicon library was diluted in a total of 75 μL of running buffer according to protocol (Oxford Nanopore Technologies 2023). The FLO-MIN114 R10.4.1 flow cell (ONT, Oxford, UK) was primed with 1000 μL of priming mixture, before loading the pooled library onto the flow cell via the SpotON sample port, following the manufacturer's protocol. The DNA library was sequenced on a MinION device for 72 h. Finally, the flow cell was sealed using a light shield and the platform lid. Nanopore sequencing was performed for 62 h (until exhaustion of the flow cell) in a darkened room, using the MinKNOW software (v23.04.6), to obtain a maximum read output. The sequenced library obtained 11.96 M reads, with an estimated N50 of 682, estimated bases of 8.69 Gb. The DNA reads are deposited in the NCBI Short Read Archive (SRA) database under accession number BioProject: PRJNA1212025.

## Basecalling and bioinformatic processing

Reads were basecalled with slow5-dorado v0.3.4, after conversion of the fast5 format to the blow5 format with slow5tools v1.1.0 to improve basecalling speed and reduce space requirements. The obtained SAM file was converted using SAMtools v1.9 and the resulting FASTQ files were demultiplexed using Porechop v0.2.4 (Wick 2017) with default settings. Quality scores of all samples were visualized and summarized using NanoPlot v1.41.6 (De Coster et al. 2018, De Coster and Rademakers 2023). Then, consensus sequences were generated using NGSpeciesID v0.3.0 (Sahlin et al. 2021) with a minimum quality threshold set to 10. The aligned threshold and mapped threshold were set to 0.6 and 0.9, respectively, as such accounting for variable error rates within reads. A polishing algorithm was also applied using the medaka option of NGSpeciesID (–medaka). NGSpeciesID employs a reference-free method to categorize reads into bins and constructs consensus sequences through iterative mapping against other reads (Sahlin et al. 2021). The advantage of using NGSpeciesID with this dataset is that any incorrectly demultiplexed reads (belonging to a different species) are segregated into a distinct consensus sequence cluster, ensuring they do not compromise the final consensus sequence (Karin et al. 2023). Following this step, table outputs containing consensus sequences from NGSpeciesID were converted to fasta files using a custom script. Next, each consensus sequence was taxonomically assigned using the blast algorithm from CREST4 v4.3.6 (Lanzén et al. 2012) with default parameters (–min_score = 155 and –score_drop = 2.0). The silvamod138pr2 database, a curated version of the SILVA NR SSU Ref. v138, was used as reference. Subsequently, the number of identified reads of each assigned taxa was determined at phylum and family level via a custom-made script. Taxa with fewer than 5 assigned reads were excluded from the dataset as a precautionary measure to prevent incorrect taxonomic assignments. Taxonomic classification of the phyla was conducted using the World Register of Marine Species (WoRMS) database (WoRMS Editorial Board, 2020).

## Data treatment and statistical analysis

Prior to downstream analyses, sequence data were normalized by rarefaction (lowest sequence depth = 3 654) using the rarefy and rrarefy function of the vegan package v2.6.6 (Oksanen et al. 2015, 2026) in R v4.3.0. Rarefaction is a normalization procedure that subsamples sequencing reads to a uniform depth across samples, allowing unbiased comparison of diversity metrics in metabarcoding datasets (e.g. Hong et al. 2022, Schloss 2024, Weiss et al. 2017). Second, we calculated the eDNA index per taxon as proposed by Kelly et al. (2019) to investigate the relationship between amplicon-based summary statistics and taxon abundance. This index rescales read-count proportions to facilitate comparisons across samples.

$$eDNA_{ij} = \frac{\frac{Y_{ij}}{\sum_i Y_{ij}}}{max_j\left(\frac{Y_{ij}}{\sum_i Y_{ij}}\right)} \quad (1)$$

where $i$ indexes species and $j$ indexes samples. Read counts were normalized within each sample to relative proportions and then scaled by the maximum proportion for each species across samples, yielding values between 0 and 1, with 1 indicating the sample in which a taxon is most relatively abundant.

We created bubble and box plots showing the relative abundance of identified taxa per sampling month and location (after rarefaction of read numbers). Next, diversity indices for each sample (after rarefaction) were calculated at the phylum level, using taxon richness (number of phyla), evenness, the Shannon–Weaver index (Shannon 1948), the Simpson index and the inverse Simpson Index (Simpson 1949) as measures of $\alpha$ diversity.

For three unicellular taxa (Ciliophora, Heterokontophyta, Myzozoa) and 5 (meso)zooplankton taxa (i.e. Annelida, Arthropoda, Chaetognatha, Ctenophora, Echinodermata, and Mollusca), we

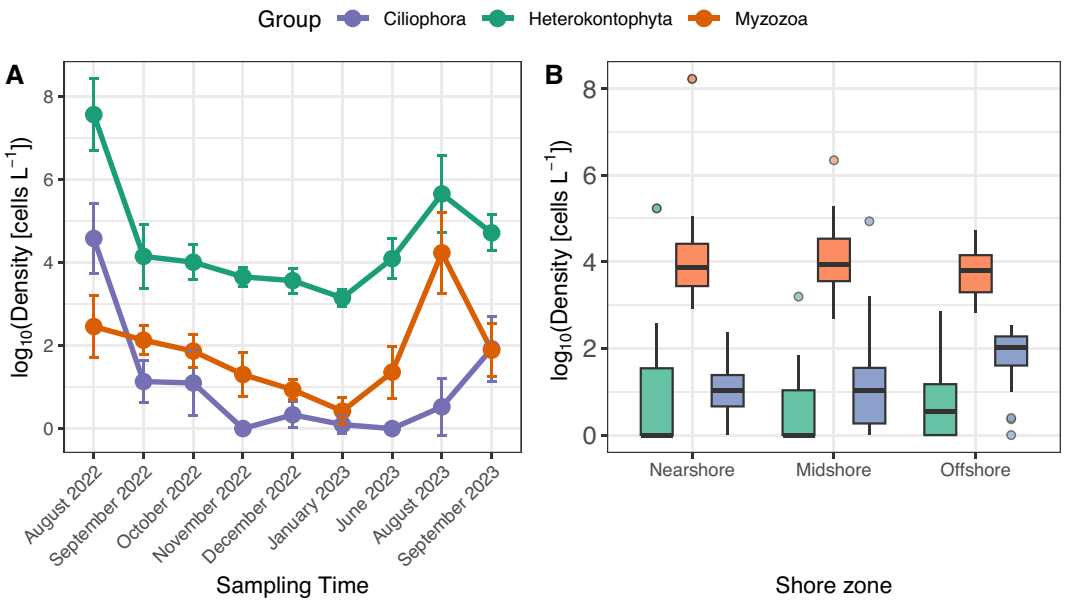


**Figure 2.** Spatiotemporal trends in the occurrence of the three major phytoplankton phyla detected using flow cytometry. (A) Temporal variation in log-transformed cell densities (cells $L^{-1}$) of the phyla throughout the study period. Data points represent the average of the summed densities of identified genera and species of each sampling station, with error bars representing the respective standard deviations. (B) Log-transformed cell densities (cells $L^{-1}$) of the same phyla across nearshore, midshore, and offshore stations of the BPNS, irrespective of sampling time. The bold horizontal line within each box indicates the median; boxes show the interquartile range (25th–75th percentile); whiskers extend to the data range (minus outliers); and dots beyond the whiskers denote outliers.

calculated correlations between relative abundance (of these taxa) of both morphological and metabarcoding approaches (using both the eDNA index and rarefaction approach). Next, we applied the Bray–Curtis index on the rarefied metabarcoding data set to estimate the degree of sample dissimilarity, an aspect of $\beta$ diversity. To test the hypothesis that plankton communities differ in time and/or space, the Bray–Curtis dissimilarity matrix was ordinated by Multidimensional Scaling (MDS) and the stress level, or measure of the goodness of fit, was calculated. Differences among community states were tested by Permutational Multivariate Analysis of Variance (PERMANOVA) with 999 permutations (Anderson 2001), implemented by the "adonis" function in the vegan package (Oksanen et al. 2015, 2026). Time of sampling and sampling location were used as predictor variables. Spearman correlation analysis was used to calculate the correlation coefficient ($R^2$) between variables. All data were visualized using the statistical computing environment R, using the packages ggplot2 v3.5.1, corrplot v0.92 and pheatmap v1.0.12.

# Results

## Reliable phylum-level taxonomic profiling via nanopore sequencing

PCR, and subsequent sequencing, was successful for 77 out of 89 samples. Additionally, no DNA was obtained from the blank samples during either extraction or PCR, suggesting that contamination was not an issue. After nanopore sequencing, processing and stringent quality filtering of the sequenced reads, we obtained on average ($\pm$ SD) 20.81 $\pm$ 0.02% of the initial reads, which were of a minimum Phred quality score of 10 for species identification (Supplementary Table S2). On average, 21 341.2 $\pm$ 13 672.1 reads were retained per sample, with an average read length and quality of 434 bp and 10.9, respectively and a N50 of 549 (Supplementary Table S2). At phylum level, on average 87.3 $\pm$ 7.8% of the reads per sample were annotated. However, at family level, on average 4.34 $\pm$ 3.58% of the reads per sample were annotated. Hence, we refrain from presenting statistical interpretation at the family level and focus in the sections below on presenting data at the phylum level. We did not find major differences between the two replicated samples (station 130, August 2022; station ZG02, December 2022) with less than one identified taxon being different between the replicates at both phylum and family level (Table S2, S3).

## Eukaryotic plankton communities: impacts of sampling method on diversity detection

The FlowCAM data was able to identify 33 species and 46 genera, belonging to 6 different phytoplankton phyla (i.e. Myzozoa (predominantly dinoflagellates), Heterokontophyta (diatoms), Ciliophora, Foraminifera and Ochrophyta). Approximately 99% of all identified phytoplankton organisms at the phylum level were diatoms. The diatom genus *Bellerochea* was the most prevalent taxon, occurring in all samples except at station 330 in July 2023. The highest cell densities were recorded at station 130 in August 2022, corresponding to a pronounced bloom of *Bellerochea* sp. ($8.7 \times 10^7$ cells $L^{-1}$), *Rhizosolenia* sp. ($5.9 \times 10^7$ cells $L^{-1}$), and *Pseudo-nitzschia* sp. ($4.4 \times 10^6$ cells $L^{-1}$) (Fig. 2).

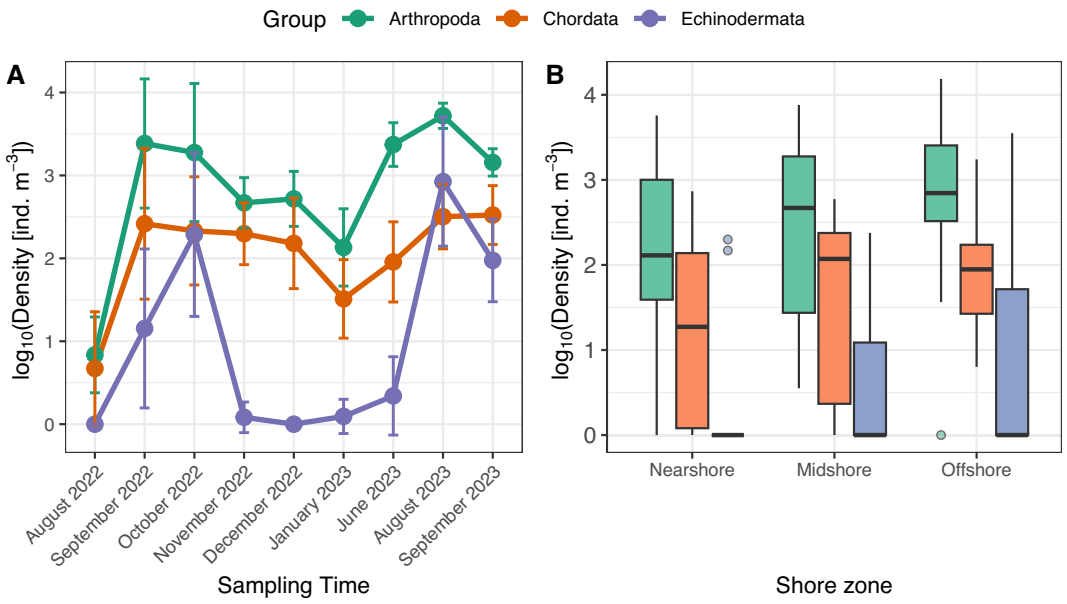


**Figure 3.** Spatiotemporal trends in the occurrence of the three major mesozooplankton phyla detected with the ZooScan. (A) Temporal variation in log-transformed plankton densities (ind $m^{-3}$) of the phyla throughout the study period. Data points represent the average of summed densities identified orders and/or genera of each sampling station, with error bars representing the respective standard deviations. (B) Log-transformed cell densities (ind $m^{-3}$) of the same phyla across nearshore, midshore, and offshore stations of the BPNS, irrespective of sampling time. The bold horizontal line within each box indicates the median; boxes show the interquartile range (25th–75th percentile); whiskers extend to the data range (except for outliers); and dots beyond the whiskers denote outliers.

Using the ZooScan, we identified eight distinct mesozooplankton phyla: Annelida, Arthropoda, Chaetognatha, Chordata, Cnidaria, Ctenophora, Echinodermata, and Mollusca. Approximately 81% of all specimens were arthropods, predominantly calanoid and harpacticoid copepods, with smaller contributions from cumaceans, amphipods, and larvae of Brachyura and Cirripedia (Fig. 3). With the exception of several samples collected in August and/or September 2022 (stations 120, 700, and 330), calanoid and harpacticoid copepods were present in all samples. About 9% of the specimens were classified as chordates, consisting mainly of appendicularians, with only few fish larvae observed. Echinoderm larvae accounted for approximately 5% of the identified specimens (Fig. 3), while chaetognaths and mollusks represented the fourth and fifth most abundant phyla, each contributing roughly 1%–2% of the total zooplankton community.

A total of 38 phyla were detected using eDNA metabarcoding, with an average of 23.4 ± 3.3 phyla identified per sample, including 25 phyla not captured by either morphological approach. Nine phyla were detected in all samples, being Arthropoda, Cercozoa, Chlorophyta, Cercozoa, Ciliophora, Cryptophyta, Heterokontophyta, Myzozoa and Oomycota (Fig. 4, S2). Myzozoa (predominantly dinoflagellates) and Heterokontophyta (predominantly diatoms) were found to be consistently the most dominant phyla in the BPNS throughout the sampling year, with average relative read abundances (after rarefaction) of 39.9 ± 12.9% and 21.6 ± 10.4%, respectively. While rarefied read counts generally indicated Myzozoa as the dominant phylum, the eDNA index often shifted the dominance towards Heterokontophyta (Fig. 5). We found no significant differences in relative read counts of both taxa in function of sampling distance to shore (Kruskal Wallis, $p > 0.05$; Fig. 5). Additionally, Arthropoda, Ciliophora, Cercozoa and Chlorophyta are also major phyla in terms of read numbers (after rarefaction), maintaining less consistent abundances throughout the years (Fig. 4), with average relative abundances of 3.1 ± 3.3, 8.4 ± 9.0%, 10.0 ± 9.0%, and 2.5 ± 3.7%, respectively. The relative contribution of the summed annotated reads of the eight most common zooplankton phyla in the BPNS (i.e. Annelida, Arthropoda, Chaetognatha, Chordata, Cnidaria, Ctenophora, Echinodermata, and Mollusca), either in their larval and/or adult stages, ranged from 0.7% to 34.1%, with an average proportion of 5.8 ± 5.4%. We also detected four fungal phyla with Ascomycota occurring most often (65/77 samples, 84%), followed by Chytridiomycota (62/77, 81%), Basidiomycota (61/77, 79%) and Zygomycota (24/77, 31%), however with low read numbers (< 6% of annotated reads of a sample).

We found no significant correlation (Spearman, $p > 0.05$) between the number of phyla detected by metabarcoding and those identified through morphological methods (summing the number of phyla detected by ZooScan and FlowCAM) (Fig. 6). Notably, eDNA metabarcoding detected at least twice as many phyla as the combined morphological approaches. For most key plankton phyla, no significant correlation (Spearman, $p > 0.05$) was observed between rarefied read counts and population densities obtained through morphological analysis (Supplementary Fig. S3). Notable exceptions included Arthropoda ($\rho = 0.52$, $p < 0.01$), Heterokontophyta ($\rho = 0.24$, $p = 0.04$), and Myzozoa ($\rho = 0.27$, $p = 0.02$). Similar patterns were found when applying the more stringent eDNA index (Supplementary Fig. S4), though under this metric, statistically significant correlations (Spearman, $p < 0.05$)

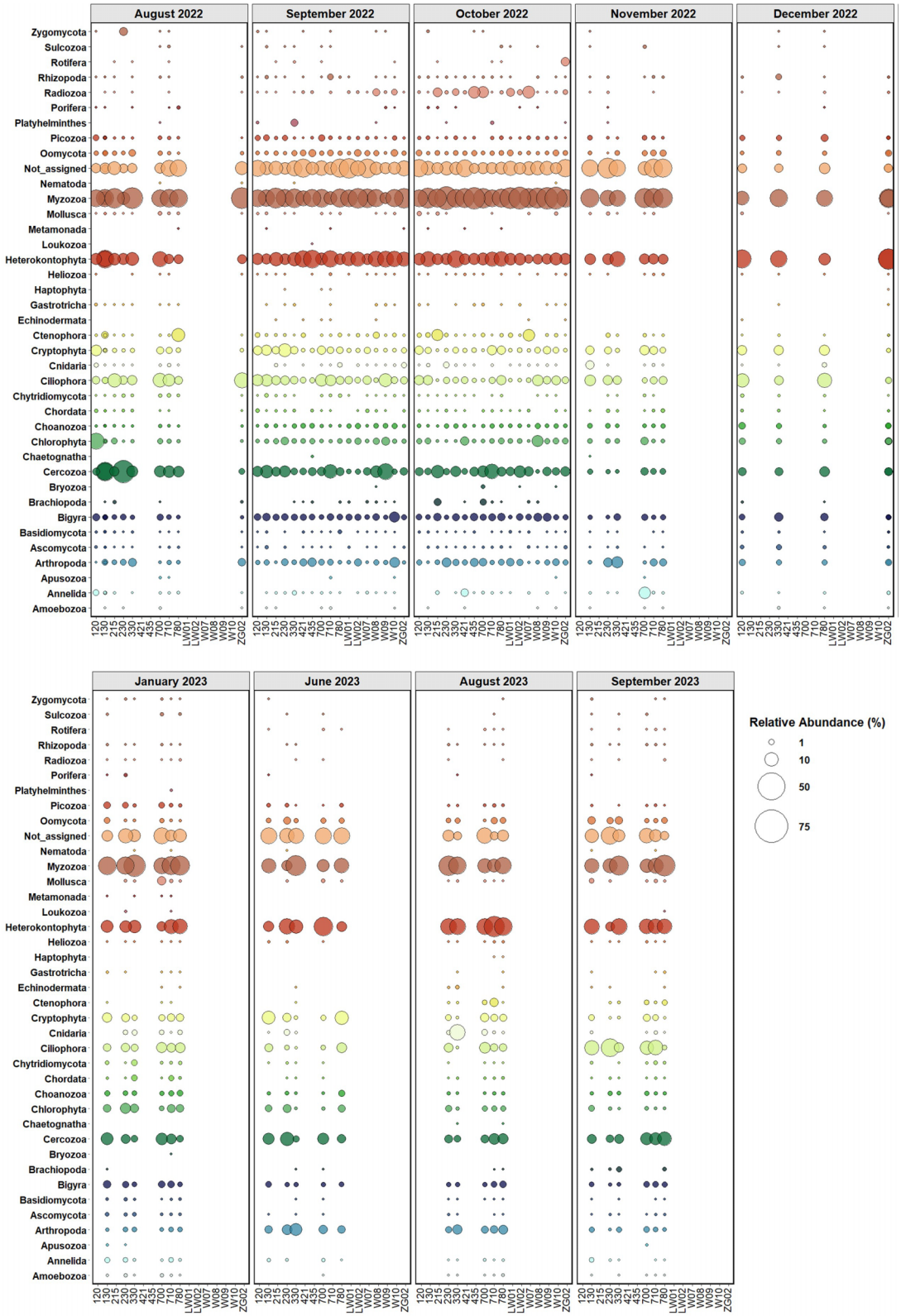


**Figure 4.** Bubble plot comparing the relative number of reads (after rarefaction) for identified phyla obtained through eDNA metabarcoding analysis among the samples. Phylum proportions for each sample sum up to 100%. Empty columns represent either failure of DNA extraction or amplification, or simply that no sample was taken on that specific sampling campaign. Samples in far offshore stations were only sampled in September and October 2022.

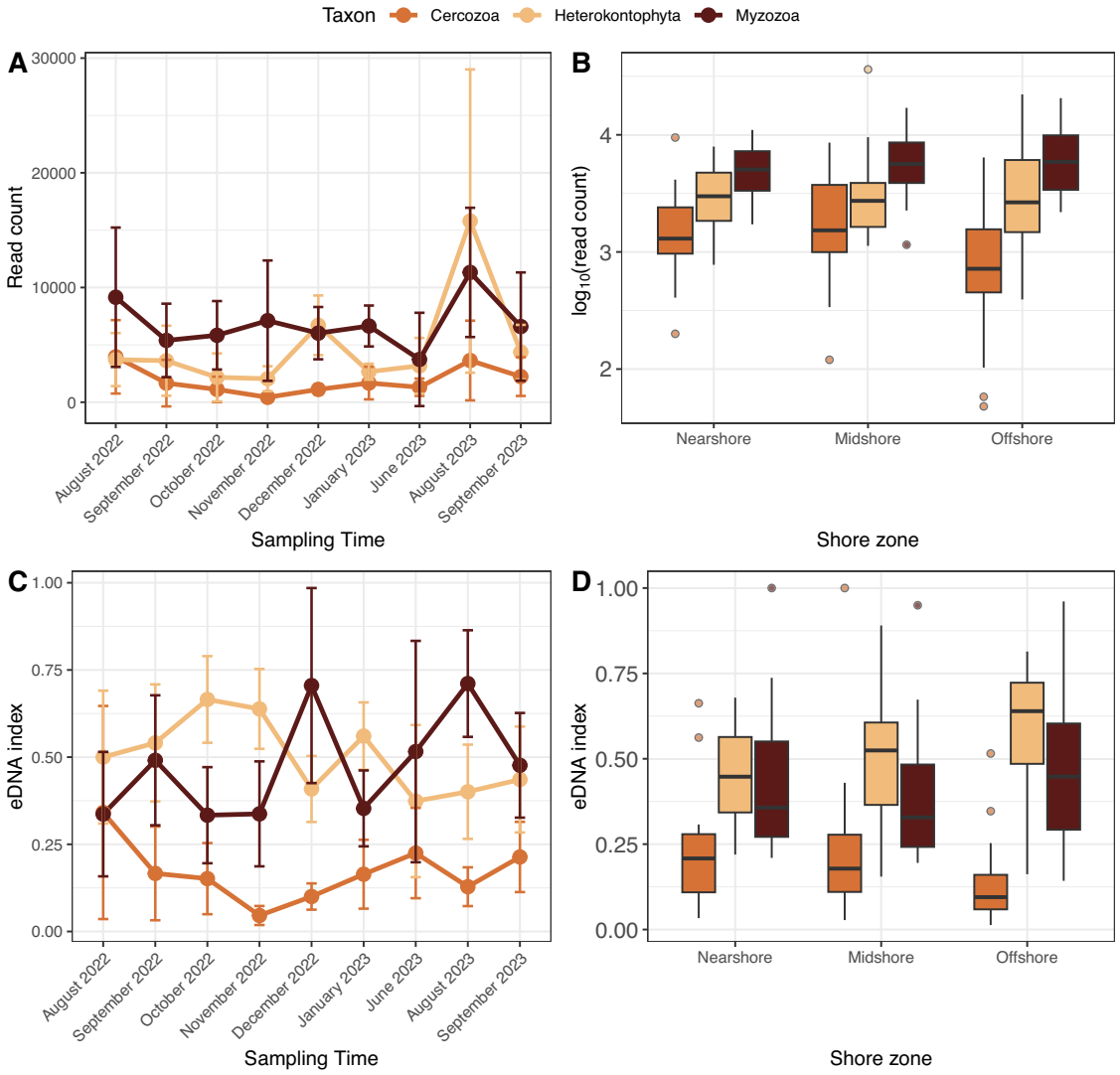


**Figure 5.** Spatiotemporal trends in the occurrence of the three major plankton phyla detected through metabarcoding. (A) Temporal variation in read counts of the phyla throughout the study period. Data points represent the average of the identified reads of each sampling station, with error bars representing the respective standard deviations. (B) Log-transformed read counts of the same phyla across nearshore, midshore, and offshore stations of the BPNS, irrespective of sampling time. The bold horizontal line within each box indicates the median; boxes show the interquartile range (25th–75th percentile); whiskers extend to the data range (minus outliers); and dots beyond the whiskers denote outliers. (C) Temporal variation in the eDNA index (*sensu* Kelly et al. 2019) for the same phyla over the study period. Values are averaged per sampling station, with error bars representing standard deviations. (D) Distribution of the eDNA index across nearshore, midshore, and offshore stations of the BPNS, irrespective of sampling time. Boxplot elements are as described in panel B.

persisted only for Arthropoda ($\rho = 0.54$, $p < 0.001$) and Myzozoa ($\rho = 0.36$, $p < 0.01$).

The detection of phyla by morphological methods and metabarcoding showed inconsistencies between approaches. For example, while Chaetognatha was identified in 34% of the zooplankton samples, it was detected through eDNA metabarcoding in only 3 samples. A same trend was observed for annelids and ctenophores, where metabarcoding detected their presence in 81 and 84% of the samples, respectively (in contrast to being counted in 12 and 10% of the zooplankton samples, respectively). Similarly, metabarcoding underestimated the presence of Echinodermata (recovered in 22% of the samples, $n = 22$) with 30% of the zooplankton samples containing echinoderm larvae. In contrast, arthropods (mostly calanoid copepods) were present in almost all zooplankton samples, while they were also detected through metabarcoding in all but one samples (99%). Chordates on the other hand were detected in 77% of the samples through barcoding, while being detected in 88% of the samples through the ZooScan.

## Eukaryotic plankton community structure and diversity estimates

Sample taxonomic diversity was estimated by calculating the rarefied phylum richness, Shannon index, (inverse) Simpson index, and Pielou's evenness. The individual Shannon and Simpson indices ranged from approximately 1.25 to 2.07 and 0.53 to 0.83, re-

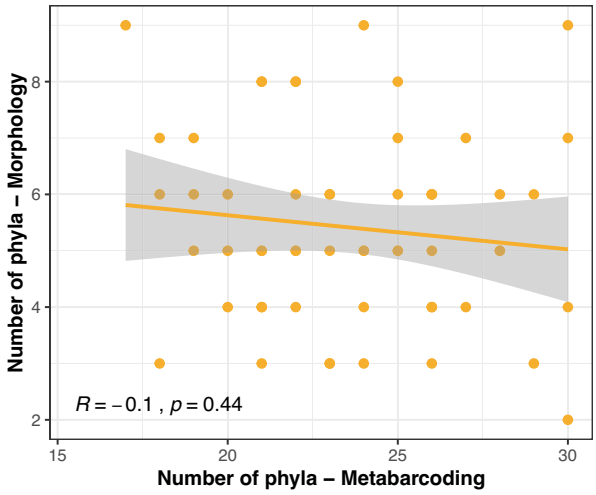


**Figure 6.** Relationship between the number of phyla identified through metabarcoding and morphological analysis (i.e. sum of phyla determined by FlowCam and ZooScan). Each point represents one sample. The orange line indicates the linear regression fit (± 95% confidence interval, shaded area). The relationship was not significant (Spearman correlation, $\rho = -0.1, p = 0.44$).

spectively (Fig. 7). Rarefied taxon richness and evenness ranged between 13.3 and 24.66 and between 0.39 and 0.76, respectively. The full table of these taxonomic diversity indices is listed in Supplementary Table S2. Fig. 7 illustrates the temporal variations in richness, Shannon and Simpson index, as well as evenness over the course of the study.

Finally, total microalgal density (FlowCAM data) showed no significant correlation with phylum number (rarefied richness; Spearman, $p > 0.05$). However, microalgal density correlated negatively with Shannon index (Spearman $\rho = -0.33$, $p < 0.01$), Simpson index (Spearman $\rho = -0.24$, $p = 0.039$), and community evenness (Spearman $\rho = -0.26$, $p = 0.024$).

## Environmental drivers of spatiotemporal variation in eukaryotic plankton communities

In order to understand how the structure of the plankton community changes over time/location, we applied Multidimensional Scaling (MDS) to the Bray–Curtis dissimilarity matrix, as a measure of Beta-diversity. The Nonmetric MDS ordination indicated no clear separation in the samples (Stress = 0.220; Fig. 8). In contrast, PERMANOVA analysis revealed that the community composition of the samples is significantly different over time (p-value = 0.001, $R^2 = 0.25$), while not over sampling location ($p = 0.057$).

Next, we aimed to determine whether seasonal variation in environmental parameters (as visualized in Fig. S5) affects plankton community structure and diversity. Supplementary Table S4 presents the summary statistics of various environmental factors used for this study. Fig. 9B summarizes significant correlations between the measured environmental variables and the calculated diversity indices. No significant correlations were found between any of the indices and fluorescence (Spearman, $p > 0.05$; Fig. 9B). Temperature correlated negatively with phylum number (rarefied richness) and evenness of the plankton community. Nutrient concentrations correlated significantly with taxon richness, Shannon and Simpson index, as well as with OBS (Spearman, $p < 0.05$). Evenness, Shannon and Simpson index correlated negatively with salinity, while the Shannon index, rarefied taxon richness (number of phyla) and the evenness correlated negatively with conductivity (Spearman, $p < 0.05$). Additionally, the relationship between environmental factors and identified phyla is illustrated through a heatmap (Fig. 9C). Hierarchical clustering reveals distinct patterns of association between the phyla and environmental conditions. The resulting two clusters of environmental parameters are (1) temperature, fluorescence, salinity and conductivity and (2) nutrient concentrations and OBS. About one third of the identified phyla (including Ciliophora, Cryptophyta, Mollusca, Picozoa and Sulcozoa) show positive correlations with nutrient concentrations, while some (e.g. Cryptophyta) are being negatively correlated with water temperature and salinity (Fig. 9C). Correlations between environmental parameters and the other phyla (including the dominant phyla Myzozoa and Heterokontophyta) tend to be less pronounced. Similar patterns were observed when examining correlations between eDNA index values at the phylum level and environmental variables (Fig. S6).

# Discussion

## MinION sequencing—potential benefits and limitations

ONT's MinION sequencer is a compact and cost-effective nanopore-based DNA sequencing device. This technology offers several significant advantages over other high-throughput sequencing platforms. It provides long-read output, has a low initial startup cost, and features straightforward and rapid library preparation protocols relative to other commercial sequencers (Pomerantz et al. 2018). Despite increasing adoption, nanopore sequencing is widely considered as error–prone, with systematic inaccuracies at single-nucleotide and motif levels, leading to consequently lower alignment efficiency compared with other next-generation sequencing platforms (Delahaye and Nicolas 2021, Sahlin and Medvedev 2021, Liu-Wei et al. 2024, Santos et al. 2025). In the current study, only 4 to 19.7% of the quality filtered reads had a Phred quality score higher of equal to 12, with an average of 8.4 ± 3.4% (Table S2). The relatively low number of reads retained after filtering may have important implications for downstream analyses. Reduced read depth likely decreased the probability of detecting rare or low-abundance taxa and may have limited the resolution of inferred community composition.

Several studies have demonstrated that data produced by the MinION are accurate enough to generate a consensus sequence for species identification with over 99% accuracy (Calus et al. 2018, Pomerantz et al. 2018, Seah et al. 2020, Srivathsan et al. 2018). However, in the current study, on average 4.34 ± 3.58% of the reads per sample were annotated at the family level (in contrast to 87.3 ± 7.8% at phylum level). Only a small fraction of detected eDNA sequences in environmental samples can usually be assigned to species level due to a lack of data and taxonomic resolution in the publicly available resources (Deiner et al. 2017, Leite et al. 2021, Zafeiropoulos et al. 2021, Bourret et al. 2023). In addition,

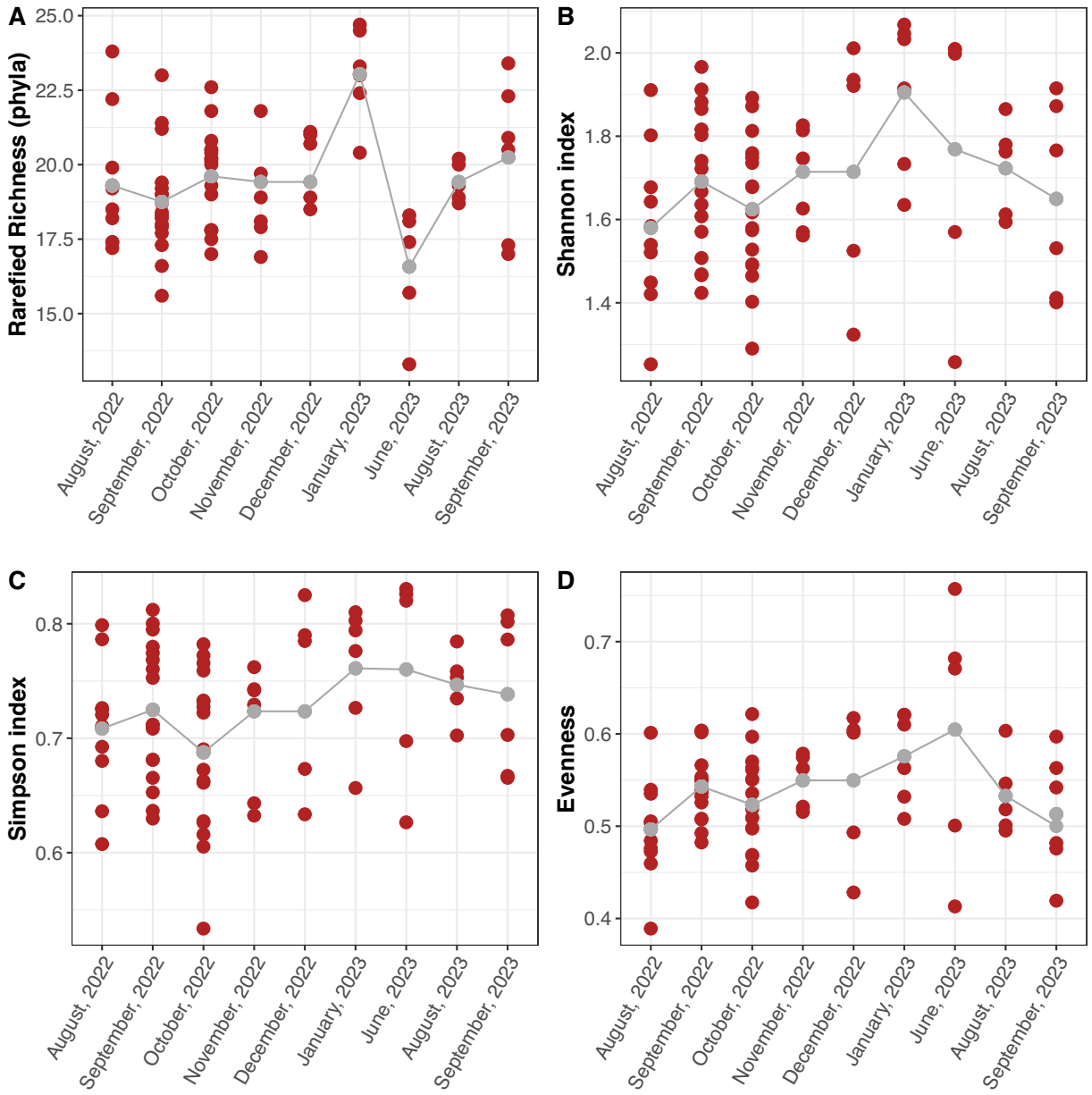


**Figure 7.** Comparison of diversity metrics through metabarcoding (based on rarefied read numbers), including (A) rarefied phylum richness, (B) Shannon index, (C) Simpson index, and (D) evenness, across different sampling time points. Red dots correspond to individual samples (sampling locations), and connecting grey dots denote monthly mean values.

higher error rates in nanopore sequencing were found to complicate accurate assignment at the species level (Winand et al. 2020, Egeter et al. 2022). To enhance taxonomic resolution and accuracy, sequencing the full length of the 18S rRNA gene could be advantageous, as it may improve differentiation among closely related taxa.

MinION sequencing also requires substantial bioinformatic processing (including the adoption of specialized basecalling and polishing pipelines), exhibits variability in flow cell performance, and shows reduced effectiveness when input DNA is fragmented or of low molecular weight (e.g. Delahaye and Nicolas 2021, Kruasuwan et al. 2024). Although continued improvements in chemistry and base calling algorithms have substantially mitigated these issues, they remain important considerations when interpreting MinION generated datasets.

## Monitoring of plankton using eDNA metabarcoding and taxonomic coverage

Using eDNA metabarcoding, we found an average of 23.4 $\pm$ 3.3 identified phyla in each sample. The number of phyla identified through metabarcoding was consistently at least twice as high as that detected using morphological approaches. Similar patterns have been reported in multiple studies on plankton communities (using different marker gene regions), which consistently show higher taxonomic diversity—at either the levels of species, genera, families, or phyla—when assessed via metabarcoding in both freshwater and marine environments (e.g. Huo et al. 2020, Chen et al. 2024, Ferreira et al. 2024, Weydmann-Zwolicka et al. 2024, Thevarajan et al. 2025). Notably, in the

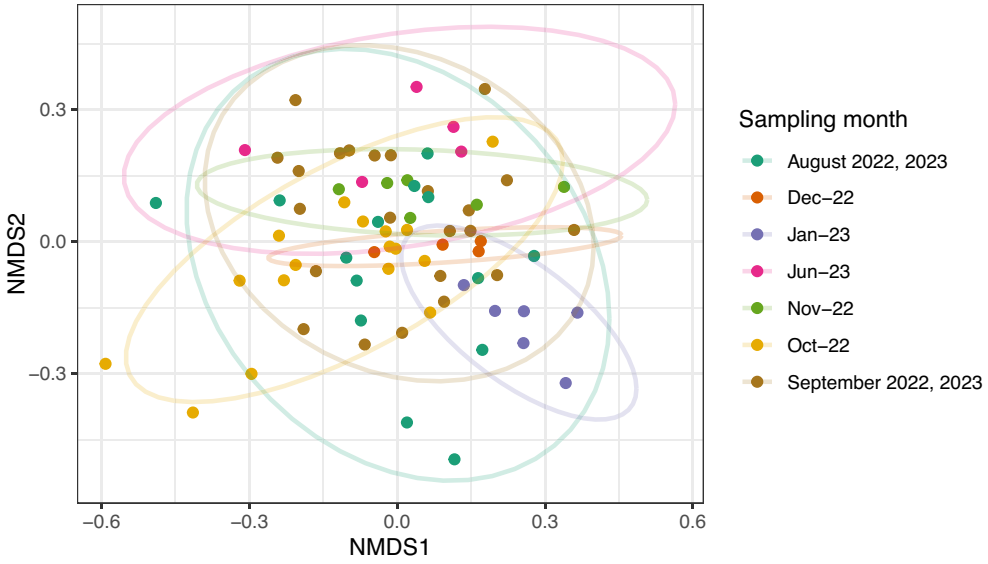


**Figure 8.** Nonmetric multidimensional scaling (MDS) plot based on Bray-Curtis dissimilarities of metabarcoding profiles (identifications at phylum level) of plankton samples collected on the BPNS. Each symbol represents one individual sample and each colour represents sampling month. The samples collected did neither cluster clearly per month, nor did samples taken at the same location (corresponding graph not shown).

present study, the morphological assessment encompassed two complementary methods—ZooScan and FlowCAM—targeting different planktonic groups (phyto- and mesozooplankton), while other groups remained undetected using these techniques. This highlights the greater efficiency and broader taxonomic coverage of eDNA metabarcoding, which can detect taxa overlooked by conventional morphological methods targeting plankton. The greater number of phyla detected through eDNA metabarcoding reflects, in part, the absence of size-selective sampling constraints; however, taxonomic resolution was largely limited to higher levels (e.g. phyla), highlighting a key limitation compared to conventional morphological approaches. However, in this study, it was not possible to identify all specimens (using morphological approaches) for all phyla due to different plankton sizes and the high taxonomic expertise required to identify all captured organisms. The overlap of the dominant phyla detected by both eDNA metabarcoding and morphological based methods, demonstrates the reliability of metabarcoding for identifying a wide range of taxa. Instances of non-overlapping detections may be attributed to the lack of corresponding species sequences in the reference databases used for taxonomic assignment (Suter et al. 2021).

Additionally, the choice of marker genes influences both the phylogenetic range of organisms detected as well as the taxonomic resolution. The 18S rRNA gene is the most widely used molecular marker for assessing eukaryotic diversity in aquatic ecosystems, including planktonic assemblages, because it is universally conserved across eukaryotes, and occurs in many copies per genome, while containing hypervariable regions that provide taxonomic resolution across a broad phylogenetic range (Pawlowski et al. et al. 2012), while the COI barcode is typically used for species level annotation of marine invertebrates (Leray et al. 2013). Our choice of 18S rRNA primers was therefore intended to target a broad range of eukaryotic taxa, including microbial eukaryotes that were otherwise not captured in this study (Balzano et al. 2015). Within the 18S rRNA gene, the V4–V5 region provides a well-established balance between taxonomic resolution, phylogenetic coverage, and amplification reliability. It enables robust discrimination across major planktonic groups, including protists, microzooplankton, and small metazoans, while remaining broadly amplifiable with universal primers (Stoeck et al. et al. 2010, Hadziavdic et al. et al. 2014). This region is widely validated in plankton metabarcoding studies and well represented in reference databases such as SILVA and the Protist Ribosomal Reference database (PR2), supporting comparable taxonomic assignments (Guillou et al. et al. 2013, Hugerth et al. et al. 2014). While the use of different markers (e.g. the COI barcode) might allow for a more targeted approach for a selection of taxa at lower resolution, approaches combining multiple primers with narrower targets remain key for capturing the full diversity of plankton (e.g. Berry et al. 2019, Novotny et al. 2025). Regardless the marker choice, the current study confirms that a complementary approach of both metabarcoding, using different markers, and morphological techniques is the best way forward to study marine biodiversity, in particular if the goal is to identify as many taxa as possible at the highest resolution.

The absence of a significant correlation between read count proportions and relative abundances for most zooplankton phyla in the BPNS in the current study agrees with some studies. Taxa with low numbers of annotated sequencing reads have been observed to correlate poorly with microscopy counts (e.g. Kelly et al. 2019, Novotny et al., 2025). Because of the low mesozooplankton densities and limited water volumes filtered, only small amounts of organismal DNA were captured. Consequently, eDNA in these samples likely originated mainly from external sources such as excreta, molts, gametes, mucus, or decaying material (Novotny et al. 2025), and therefore may not directly reflect population biomass (Kirtane et al. 2021). For example, based on rarefied read counts, the phylum Myzozoa appeared the dominant plankton phylum, whereas diatoms were more abundant (cell density) according to morphological observations. However, the densities of the dominant phyla—diatoms, dinoflagellates, and arthropods—showed significant correlations with the annotated read counts

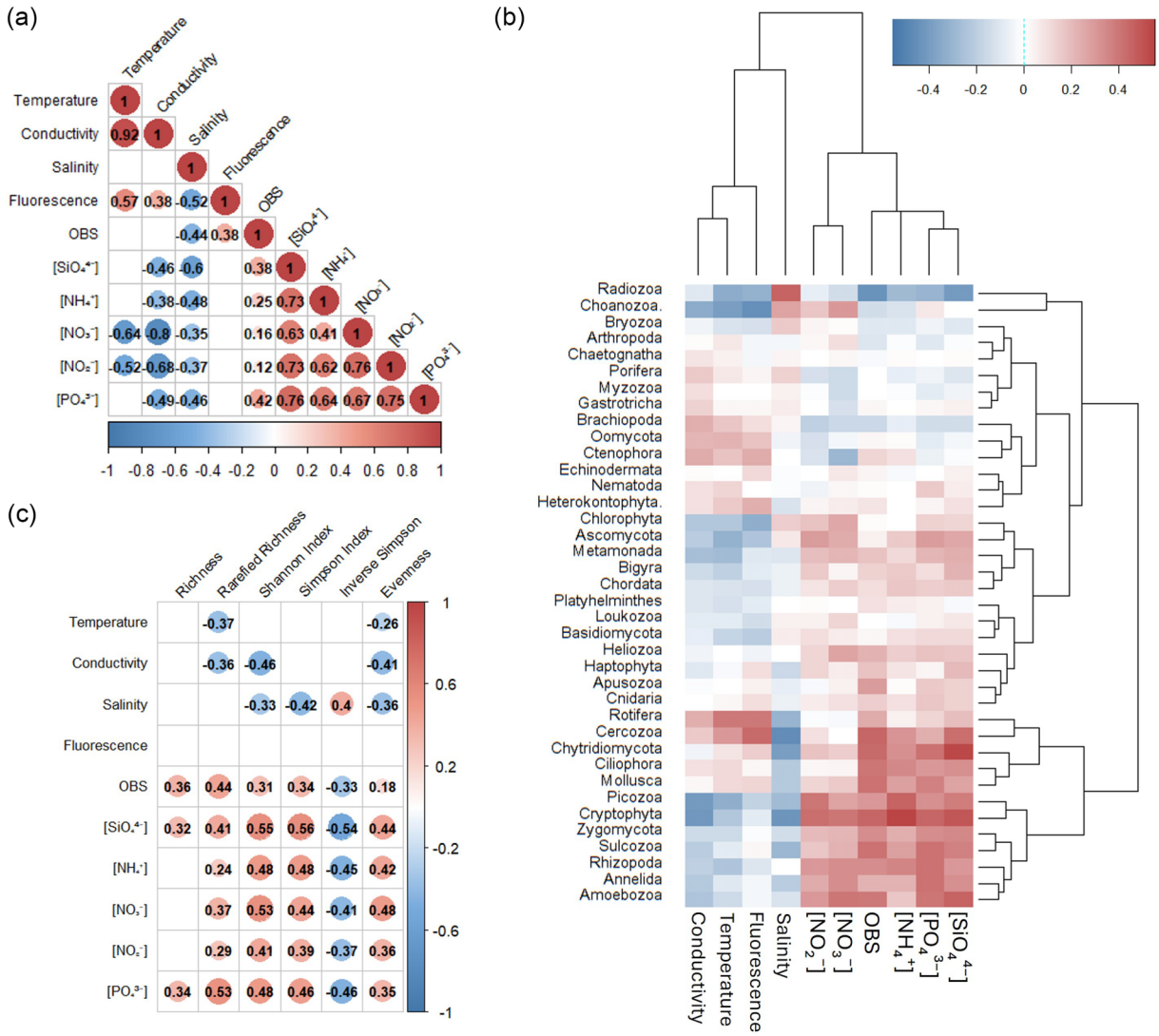


**Figure 9.** Graphs depicting relationships between taxonomic diversity and environmental parameters of plankton on the BPNS. (a) Correlation plot visualising correlations (Spearman) between the environmental variables. The circles' colour represent correlation strength, while the numbers inside each box indicate *p*-value. Only significant correlations are reported ($p < 0.05$), while insignificant correlation coefficient values are left blank. (b) Correlation plot visualising correlations (Spearman) between the calculated diversity indices and the environmental parameters. The interpretation remains consistent with the explanation provided for graph A. (c) Heatmap illustrating the Spearman correlation between the rarefied read counts of the phyla and the environmental parameters. The rows correspond to phyla, while the columns represent environmental factors. The dendrogram on the top and right sides of the heatmap illustrate the hierarchical clustering of the environmental factors and taxa, respectively, based on their Euclidean distance.

(after rarefaction) obtained from eDNA metabarcoding in the current study.

However, discrepancies became apparent when the same data were expressed as an eDNA index (Fig. 5). Despite the use of rarefied read counts, which control for sequencing depth, the eDNA index applies an additional within-sample standardization that rescales taxa relative to the total community signal. This transformation can reduce the apparent dominance of taxa such as Myzozoa when their high read proportions are driven by uneven community composition or taxon-specific amplification efficiency, rather than proportional ecological dominance. Consequently, taxa that appear dominant in rarefied read counts may lose prominence in the eDNA index, while others with more balanced representation across samples become relatively more important. This highlights that, even after rarefaction, different data transformations can lead to contrasting interpretations of community structure, and should therefore be considered carefully when linking metabarcoding results to ecological patterns.

Regardless, several zooplankton studies focusing on DNA metabarcoding, rather than eDNA obtained from water samples, also found positive correlations between the abundance of morphological taxa of macroinvertebrates and the relative read number after rarefaction (e.g. Yang et al. 2017, Serrana et al. 2019, Semmouri et al. 2021). The two approaches—"bulk DNA metabarcoding" and "eDNA metabarcoding"—represent points along a continuum of DNA sampling strategies, ranging from coarse filters with large water volumes to fine filters with smaller volumes (Suter et al. 2021, Taberlet et al. 2012, Taberlet, Bonin and Zinger 2018). However, the ease of sampling eDNA, and the possibility of standardized sampling kits, make it possible to increase sampling in-

tensity and temporal and spatial resolution substantially. Additionally, by not specifically selecting for mesozooplankton, filtered water samples allow for simultaneous analysis of other functional groups spanning a large size spectrum (Takahashi et al. 2023). Moreover, in some instances, we detected zooplankton through eDNA metabarcoding while the corresponding organisms were not present in the zooplankton samples. Future work should examine whether these patterns persist during spring phytoplankton blooms, when high cell densities may obscure rare species—a limitation we could not address here.

## Eukaryotic plankton community structure and diversity

In this study, it was not possible to identify all specimens for all phyla due to different plankton sizes and the high taxonomic expertise required to identify all captured organisms. Moreover, the taxonomic resolution achieved by metabarcoding in the present study was insufficient to support reliable inferences below the phylum level; therefore, the subsequent discussion is primarily confined to this taxonomic rank. Consequently, this study also explored taxonomic diversity patterns at a notably broad taxonomic scale—the phylum level—contrasting with the majority of studies that typically assess diversity at the species or order level, focusing on the dominant taxa. At a similar level, Perneel et al. (2024) provided a comprehensive year-long metatranscriptomic dataset from the BPNS. Their findings, which corroborate those of the present study (in terms of read numbers), indicate that diatoms and dinoflagellates are the dominant taxa within the plankton community and are present throughout the year. Lefebvre et al. (2011) and Hernández-Fariñas et al. (2014) also reported that the phytoplankton community in the eastern English Channel and the Southern Bight of the North Sea is predominantly composed of diatoms, dinoflagellates, and Prymnesiophyceae (Haptophyta), which together account for 81% of the total abundance. Flow cytometry data confirmed the presence of the diatom *Bellerochea* sp. throughout the year, with a distinct bloom occurring in August, consistent with the observations of Mortelmans et al. (2024). In contrast, *Thalassiosira* species did not exhibit a bloom in June, unlike the patterns reported by Liu et al. (2025) for 2018 and 2019. These authors also documented an earlier *Thalassiosira* bloom (May) in 2021, suggesting changes in the taxon's phenology. As samples from May were not available in the present study, we were unable to determine whether a similar early bloom occurred in the year of sampling, which could explain the missing peak in the current dataset.

Perneel et al. (2024) reported successive assemblages of diatom species over time. However, due to the lower taxonomic resolution of our metabarcoding dataset, we were unable to confirm these patterns through metabarcoding analysis. Nevertheless, similar patterns were observed between metabarcoding read counts and morphologically derived cell densities for diatoms and dinoflagellates (Fig. 2 and 5). In addition, Perneel et al. (2024) reported seasonality in other taxa as well, with certain taxonomic groups being restricted to specific months; for example, elevated abundances of ctenophores (specifically *Mnemiopsis leidyi*) were observed in August. This observation aligns with the increased read ctenophore counts observed in samples collected during August, September, and October in the current study. The late summer bloom of the invasive ctenophore *M. leidyi* was already established by Vansteenbrugge et al. (2015b). Notably, seasonal variation in arthropod densities was observed in the ZooScan data, with copepods, which are typically present year-round, being absent from several samples collected in August 2022. These copepod depletions coincided with a period of elevated temperatures, as extensively documented by Semmouri et al. (2023) and Mortelmans et al. (2024). Among the detected phyla, we also discriminated four fungal lineages, among which Chytridiomycota. Chytrids are one of the dominating fungal phyla in coastal regions worldwide (e.g. Debeljak and Baltar 2023, Peng et al. 2024). We are the first study, as far as we know, to report the presence of marine fungi in this region, although some studies have been reporting the presence of marine fungi in the northern part of the North Sea (e.g. Meyers et al. 1967, Kumar et al. 2018). Future research is needed to investigate marine fungal diversity at finer taxonomic resolutions and to elucidate taxon-specific spatiotemporal dynamics. Several other rarer phyla (e.g. Picozoa, Loukozoa) have also not yet been studied in this region and remain to be further documented.

Although several studies have validated the breadth and diversity of taxa detected through metabarcoding (e.g. Djurhuus et al. 2018, Suter et al. 2021), there is still no consensus on its quantitative application, particularly for studying seasonal dynamics or changes in zooplankton biomass over time. In the current study, taxonomic diversity of the samples was estimated by calculating diversity indices, such as the Shannon index and Simpson indices. Our diversity estimates for the pelagic plankton community (Table S3) are similar to those reported by other studies. For example, Ibarbalz et al. (2019) investigated global trends in marine plankton diversity from 12 marine areas across the world (*Tara* Oceans) and reported Shannon Indices ranging between 0.11 and 7.001 across all kingdoms of life. The diversity indices in the current study were calculated from the rarefied read numbers of each taxon. However, there are several challenges that impede from accurately estimating taxon abondance through eDNA metabarcoding due to several factors in both the field and the laboratory (Kelly 2016). In the field, the copy number of DNA arising from an individual in an environmental sample is influenced by several parameters, such as its origin, state (quality), fate and transport processes (e.g. Barnes and Turner 2016). For example, different eDNA shedding rates, or the organism's size can strongly influence detection (e.g. Sassoubre et al. 2016). This may partially account for the discrepancy between the barcoding and morphological analysis in the current study, which indicated Myzozoa and Heterokontophyta as the dominant phylum, respectively. Moreover, Lapeyra Martin, Santi and Pitta (2022) emphasized that metabarcoding can overrepresent taxa with high rRNA gene copy numbers (e.g. dinoflagellates compared to diatoms), which may inflate apparent dominance and reduce perceived richness. High variability in 18S rRNA gene copy number can indeed quickly reduce the correspondence between DNA read counts and actual organism abundances (Gong & Marchetti 2019). The dominance of dinoflagellates and associated biases in microalgal metabarcoding have been widely documented (e.g. Song et al. 2019, Liu et al. 2020, Cui et al. 2021, Xu, Yu and Cheng 2016). Consequently, many studies take a more cautious approach, using DNA metabarcoding primarily to detect species presence or assess frequencies of occurrence (Jensen et al. 2022). In the laboratory, primer bias driven by mismatches with their target has been shown to skew the relative abundance of amplified DNA from mock communities (e.g. Piñol

et al. 2014). Similarly, the same mechanism might alter the relative abundance of a species' DNA amplified from eDNA. Primer bias results in an increased variance in read abundance observed relative to their true abundance in an environmental sample, on top of the amplifying nature of the PCR process itself. Together, the combination of primer bias, library preparation procedures and the amplification process itself can cause a large variance in reads observed for any given species and prevent the detection of rare species altogether. We therefore examined whether diversity indices correlated with microalgal cell densities (used as a proxy for phytoplankton blooms, data derived from FlowCAM data). No correlation was observed between total (summed) cell densities and taxon richness (number of phyla). However, this pattern is not universal. Jacobs-Palmer et al. (2021), for example, applied eDNA metabarcoding in Hood Canal (Puget Sound, USA) and found that harmful algal taxa (e.g. *Pseudo-nitzschia*, *Alexandrium*, *Karlodinium*) often dominated samples, reducing the detectability of other taxa. However, we observed significant negative correlations between phytoplankton cell densities and diversity indices, including measures of evenness (Shannon, Simpson, and Evenness). In the study of Jacobs-Palmer et al. (2021), high read counts of harmful taxa were indeed often associated with low community evenness and diversity. Similarly, diversity indices dropped as a few dinoflagellate taxa became highly abundant during bloom periods in Liu et al. (2020).

## Environmental drivers of plankton diversity

Our environmental analysis (Fig. 5) revealed significant correlations among environmental factors. We observed several positive correlations between diversity indices, such as the Shannon and Simpson index, and particularly nutrients such as nitrate ($NO_3^-$) and silicate ($SiO^{4-}$). The latter likely align with enhanced phytoplankton diversity and metabolic activity, and by consequence primary consumers, such as zooplankton. Previous studies already established a positive correlation between nutrient concentrations and algal densities, or their pigment content (e.g. Semmouri et al. 2024b, Groß et al. 2022). Additionally, higher OBS values, pointing to increased turbidity, were found to correlate positively with the diversity indices, probably a consequence of increased concentrations of suspended particulate matter (Downing et al. 1981), including phytoplankton. Surprisingly, we found few significant correlations between any diversity index and water temperature, reflecting a non-linear relationship between temperature and organismal responses (e.g. Semmouri et al. 2024b). Similarly, Desmit et al. (2019) found no significant relationship between chlorophyll concentration variability and sea surface temperatures (SST) in the Southern and Central North Sea using a long time series spanning four decades (1975–2015). This is likely the result of a nonlinear relation between the two variables, as has been demonstrated for example for copepod abundance in this region as well (Semmouri et al. 2023).

Apart from the lower taxonomic resolution, resulting from the application of nanopore sequencing, other limitations of this study are (1) the gap in the time series coinciding with the typical spring bloom in the pelagic, and (2) the temporal resolution of the sampling campaigns, which may overlook more fine-scale dynamics and rapid environmental fluctuations that can occur between the monthly sampling intervals. Higher-frequency sampling could provide more detailed insights into the short-term drivers of phytoplankton dynamics, especially during critical transition periods in bloom development.

# Conclusion

Overall, while eDNA targeting the V4–V5 region of the 18S rRNA gene enables the analysis of a broad and heterogeneous range of organisms and detected more phyla than the two morphology-based techniques combined, several limitations were observed. Not all taxa were detected by metabarcoding, and the resolution of the applied marker was relatively low. Furthermore, the high error rates associated with nanopore sequencing restricted taxonomic annotation mainly to the phylum and family levels. In addition, the high variability in 18S rRNA gene copy number likely weakened the correspondence between DNA read counts and actual organism abundances, leading to the apparent, but erroneous, dominance of dinoflagellates in the community profile. The diatom *Bellerochea* was the dominant phytoplankton taxon throughout the year, indicating its establishment as a novel bloom-forming species in the southern North Sea. As sampling did not occur during the spring bloom, species detection—based on eDNA metabarcoding—did not seem to be affected by phytoplankton cell densities. However, the metabarcoding data failed to capture the seasonal dynamics of zooplankton taxa present throughout the year. In summary, our study represents an important step toward documenting less-studied taxa, which is essential for detecting future shifts or changes in community dynamics and provides a valuable baseline for subsequent biodiversity research.

# Acknowledgements

The authors extend their gratitude to the Flanders Marine Institute (VLIZ) and the LifeWatch project, a Flemish contribution to the LifeWatch ESFRI led by VLIZ, for their invaluable support. Special thanks are owed to Jonas Mortelmans (VLIZ), and the crew of R/V *Simon Stevin* for technical assistance on board. We thank Jolien Depecker, Lisa Vanderstraeten, Nancy De Saeyer and Emmy Pequeur for technical assistance. IS was awarded a BOF postdoctoral fellowship (BOF24/PDO/026) by Ghent University.

# Authors' contributions

Funding was obtained by Jana Asselman and Filip Volckaert. Resources were provided by Colin Janssen, Jana Asselman and Filip Volckaert. All authors contributed to the conception and design of the study. Material preparation, data collection and analysis were performed by Michiel De Cooman and Enora Geslain under the lead of Ilias Semmouri. The first draft of the manuscript was written by Ilias Semmouri. Editing and reviewing of the manuscript was done by all authors. All authors read and approved the final manuscript.

## Supplementary data

Supplementary data is available at *ICES Journal of Marine Science* online.

## Conflicts of interest

The authors declare that the research was conducted in the absence of any commercial or financial relationships that could be construed as a potential conflict of interest.

## Funding

The research leading to the data presented in this publication was carried out within a joint development action by EMBRC nodes funded by EMBRC Belgium—FWO project FWOIRI2021000202. Computational resources, facilitated through the Stevin Supercomputer Infrastructure, and services used in this study were made possible by the VSC (Flemish Supercomputer Center), which receives funding from Ghent University, FWO, and the Flemish Government's department of EWI.

## Data availability

The high-quality DNA reads are deposited in the NCBI Short Read Archive (SRA) database under accession number BioProject: PRJNA1212025. All other datasets generated and analyzed for this study are included in the article/Supplementary material.

## References

Álvarez E, López-Urrutia Á, Nogueira E *et al.* How to effectively sample the plankton size spectrum? A case study using FlowCAM. *J Plankton Res* 2011;**33**:1119–33. https://doi.org/10.1093/plankt/fbr012

Amadei Martínez L, Mortelmans J, Dillen N *et al.* LifeWatch observatory data: phytoplankton observations in the Belgian Part of the North Sea. *Biodiversity Data Journal* 2020;**8**:e57236. https://doi.org/10.3897/BDJ.8.e57236

Ames CL, Ohdera AH, Colston SM *et al.* Fieldable environmental DNA sequencing to assess jellyfish biodiversity in nearshore waters of the Florida Keys, United States. *Frontiers in Marine Science* 2021;**8:640527**. https://doi.org/10.3389/fmars.2021.640527

Anderson MJ. A new method for non-parametric multivariate analysis of variance: non-parametric manova for ecology. *Austral Ecol*. 2001;**26**:32–46. https://doi.org/10.1111/j.1442-9993.2001.01070.pp.x

Balzano S, Abs E, Leterme SC. Protist diversity along a salinity gradient in a coastal lagoon. *Aquat Microb Ecol*, 2015;**74**:263–77. https://doi.org/10.3354/ame01740

Barnes MA, Turner CR. The ecology of environmental DNA and implications for conservation genetics. *Conservation Genetics*, 2016;**17**:1–17. https://doi.org/10.1007/s10592-015-0775-4

Berry TE, Saunders BJ, Coghlan ML *et al.* Marine environmental DNA biomonitoring reveals seasonal patterns in biodiversity and identifies ecosystem responses to anomalous climatic events. *PLos Genet* 2019;**15**:e1007943. https://doi.org/10.1371/journal.pgen.1007943

Bourret A, Nozères C, Parent E *et al.* Maximizing the reliability and the number of species assignments in metabarcoding studies using a curated regional library and a public repository. *Metabarcoding and Metagenomics* 2023;**7**:e98539. https://doi.org/10.3897/mbmg.7.98539

Brooks TM, Butchart SHM, Cox NA *et al.* Harnessing biodiversity and conservation knowledge products to track the Aichi Targets and Sustainable Development Goals. *biodivers* 2015;**16**:157–74. https://doi.org/10.1080/14888386.2015.1075903

Bucklin A, Peijnenburg KTCA, Kosobokova KN *et al.* Toward a global reference database of COI barcodes for marine zooplankton. *Mar Biol* 2021;**168**:78 https://doi.org/10.1007/s00227-021-03887-y

Calus ST, Ijaz UZ, Pinto AJ. NanoAmpli-Seq: a workflow for amplicon sequencing for mixed microbial communities on the nanopore sequencing platform. *GigaScience*, 2018;**7**:giy140. https://doi.org/10.1093/gigascience/giy140

Chen X, Wei Q, Niu Y *et al.* Complementary roles of eDNA metabarcoding and microscopy in plankton monitoring across seven habitats. *J Plankton Res* 2024;**46**:555–66. https://doi.org/10.1093/plankt/fbae052

Chiba S, Batten S, Martin C *et al.* Zooplankton monitoring to contribute towards addressing global biodiversity conservation challenges. *J Plankton Res* 2018;**40**:509–18. https://doi.org/10.1093/plankt/fby030

Creer S, Deiner K, Frey S *et al.* The ecologist's field guide to sequence-based identification of biodiversity. *Methods Ecol Evol* 2016;**7**:1008–18. https://doi.org/10.1111/2041-210X.12574

Cui Z, Xu Q, Gibson K *et al.* Metabarcoding analysis of harmful algal bloom species in the Changjiang Estuary, China. *Sci Total Environ* 2021;**782**:146823. https://doi.org/10.1016/j.scitotenv.2021.146823

Debeljak P, Baltar F. Fungal diversity and community composition across ecosystems. *J Fungi*, 2023;**9**:510. https://doi.org/10.3390/jof9050510

De Coster W, D'Hert S, Schultz DT *et al.* NanoPack: visualizing and processing long-read sequencing data. *Bioinformatics* 2018;**34**:2666–9. https://doi.org/10.1093/bioinformatics/bty149

De Coster W, Rademakers R. NanoPack2: population-scale evaluation of long-read sequencing data. *Bioinformatics*, 2023;**39**:btad311. Doi: https://doi.org/10.1093/bioinformatics/btad311

Deiner K, Bik HM, Mächler E *et al.* Environmental DNA metabarcoding: transforming how we survey animal and plant communities. *Mol Ecol* 2017;**26**:5872–95. https://doi.org/10.1111/mec.14350

Delahaye C, Nicolas J. Sequencing DNA with nanopores: troubles and biases. *PLoS One*, 2021;**16**:e0257521. https://doi.org/10.1371/journal.pone.0257521

Desmit X, Nohe A, Borges AV *et al.* Changes in chlorophyll concentration and phenology in the North Sea in relation to de-eutrophication and sea surface warming. *Limnol Oceanogr* 2019;**65**:828–47 https://doi.org/10.1002/lno.11351

Djurhuus A, Pitz K, Sawaya NA *et al.* Evaluation of marine zooplankton community structure through environmental DNA metabarcoding. *Limnology and Oceanography: Methods* 2018;**16**:209–21. https://doi.org/10.1002/lom3.10237

Doğan O, Örün AD, Bilgin R *et al.* Using eDNA metabarcoding to capture a snapshot of plankton community composition in the western Marmara Sea and northeastern Aegean Sea. *Mar Biodivers* 2025;**55**: 60. https://doi.org/10.1007/s12526-025-01544-x

Downing JP, Sternberg R, Lister C. New instrumentation for the investigation of sediment suspension processes in the shallow marine environment. *Mar Geol*, 1981;**42**:19–34. https://doi.org/10.1016/0025-3227(81)90156-0

Egeter B, Veríssimo J, Lopes-Lima M *et al.* Speeding up the detection of invasive bivalve species using environmental DNA: a Nanopore and Illumina sequencing comparison. *Mol Ecol Resour* 2022;**22**:2232–47. https://doi.org/10.1111/1755-0998.13610

Ferdous Z, Muktadir A. A review: potentiality of zooplankton as bioindicator. *American Journal of Applied Sciences* 2009;**6**:1815–9.

Ferreira AO, Azevedo OM, Barroso C *et al.* Multi-marker DNA metabarcoding for precise species identification in ichthyoplankton samples. *Sci Rep* 2024;**14**:19772. https://doi.org/10.1038/s41598-024-69963-7

Flanders Marine Institute (VLIZ), Belgium LifeWatch observatory data: monthly CTD temperature and salinity measurements in the Belgian Part of the North Sea. 2024a. https://rshiny.lifewatch.be/ctd-data/ (15 March 2026, date last accessed)

Flanders Marine Institute (VLIZ), Belgium LifeWatch observatory data: nutrient, pigment, suspended matter and Secchi measurements in the Belgian Part of the North Sea. 2024b. https://doi.org/10.14284/441

Gong W, Marchetti A. Estimation of 18S gene copy number in marine eukaryotic plankton using a Next-Generation sequencing approach. *Frontiers in Marine Science*, 2019;**6**:219. https://doi.org/10.3389/fmars.2019.00219

Grandremy N, Dupuy C, Petitgas P *et al.* The ZooScan and the ZooCAM zooplankton imaging systems are intercomparable: a benchmark on the Bay of Biscay zooplankton. *Limnology and Oceanography: Methods* 2023;**21**:718–33. https://doi.org/10.1002/lom3.10577

Groß E, Di Pane J, Boersma M *et al.* River discharge-related nutrient effects on North Sea coastal and offshore phytoplankton communities. *J Plankton Res* 2022;**44**:947–60. https://doi.org/10.1093/plankt/fbac049

Guillou L, Bachar D, Audic S *et al.* The Protist Ribosomal Reference database (PR2): a catalog of unicellular eukaryote small sub-unit rRNA sequences with curated taxonomy. *Nucleic Acids Res* 2013;**41**:D597–604. https://doi.org/10.1093/nar/gks1160

Hadziavdic K, Lekang K, Lanzen A *et al.* Characterization of the 18S rRNA gene for designing universal eukaryote specific primers. *PLoS One* 2014;**9**:e87624. https://doi.org/10.1371/journal.pone.0087624

Hendricks A, Mackie CM, Luy E *et al.* Compact and automated eDNA sampler for in situ monitoring of marine environments. *Sci Rep* 2023;**13**:5210. https://doi.org/10.1038/s41598-023-32310-3

Hernández-Fariñas T, Soudant D, Barillé L *et al.* Temporal changes in the phytoplankton community along the French coast of the eastern English Channel and the southern Bight of the North Sea. *ICES J Mar Sci* 2014;**71**:821–33, https://doi.org/10.1093/icesjms/fst192

Hong J, Karaoz U, De Valpine P *et al.* To rarefy or not to rarefy: robustness and efficiency trade-offs of rarefying microbiome data. *Bioinformatics* 2022;**38**:2389–96. https://doi.org/10.1093/bioinformatics/btac127

Hugerth LW, Muller EEL, Hu YOO *et al.* Systematic design of 18S RRNA gene primers for determining eukaryotic diversity in microbial consortia. *PLoS One* 2014;**9**:e95567. https://doi.org/10.1371/journal.pone.0095567

Huo S, Li X, Xi B *et al.* Combining morphological and metabarcoding approaches reveals the freshwater eukaryotic phytoplankton community. *Environmental Sciences Europe* 2020;**32**:37. https://doi.org/10.1186/s12302-020-00321-w

Ibarbalz F, Henry N, Brandão M *et al.* Global trends in marine plankton diversity across kingdoms of life. *Cell* 2019;**179**:1084–1097.e21. https://doi.org/10.1016/j.cell.2019.10.008

Jacobs-Palmer E, Gallego R, Cribari K *et al.*. Environmental DNA Metabarcoding for Simultaneous Monitoring and Ecological Assessment of Many Harmful Algae. *Frontiers in Ecology and Evolution* 2021;**9**. https://doi.org/10.3389/fevo.2021.612107

Jensen MR, Sigsgaard EE, De Paula Ávila M *et al.* Short-term temporal variation of coastal marine eDNA. *Environmental DNA* 2022;**4**:747–62. https://doi.org/10.1002/edn3.285

Karin BR, Arellano S, Wang L *et al.* Highly-multiplexed and efficient long-amplicon PacBio and Nanopore sequencing of hundreds of full mitochondrial genomes. *Bmc Genomics [Electronic Resource]* 2023;**24**:229. https://doi.org/10.1186/s12864-023-09277-6

Keck F, Couton M, Altermatt F. Navigating the seven challenges of taxonomic reference databases in metabarcoding analyses. *Mol Ecol Resour* 2023;**23**:742–55. https://doi.org/10.1111/1755-0998.13746

Kelly RP. Making environmental DNA count. *Mol Ecol Resour*, 2016;**16**:10–2. https://doi.org/10.1111/1755-0998.12455

Kelly RP, Port JA, Yamahara KM *et al.* Using environmental DNA to census marine fishes in a large mesocosm. *PLoS One* 2014;**9**:e86175. https://doi.org/10.1371/journal.pone.0086175

Kelly RP, Shelton AO, Gallego R. Understanding PCR processes to draw meaningful conclusions from environmental DNA Studies. *Sci Rep*, 2019;**9**:12133. https://doi.org/10.1038/s41598-019-48546-x

Kessler A, Goris N, Lauvset SK, Observation-based Sea surface temperature trends in Atlantic large marine ecosystems. *Progress in Oceanography*, 2022;**208**:102902–. https://doi.org/10.1016/j.pocean.2022.102902

Kiørboe T. Formation and fate of marine snow: small-scale processes with large-scale implications. *Scientia Marina*, 2001;**65**:57–71. https://doi.org/10.3989/scimar.2001.65s257

Kirtane A, Wieczorek D, Noji T *et al.* Quantification of Environmental DNA (eDNA) shedding and decay rates for three commercially harvested fish species and comparison between eDNA detection and trawl catches. *Environmental DNA* 2021;**3**:1142–55. https://doi.org/10.1002/edn3.236

Kruasuwan W, Sawatwong P, Jenjaroenpun P *et al.* Comparative evaluation of commercial DNA isolation approaches for nanopore-only bacterial genome assembly and plasmid recovery. *Sci Rep* 2024;**14**:27672. https://doi.org/10.1038/s41598-024-78066-2

Kumar A, Sørensen JL, Hansen FT *et al.* Genome sequencing and analyses of two marine Fungi from the North Sea unraveled a plethora of novel biosynthetic gene clusters. *Sci Rep* 2018;**8**:10187. https://doi.org/10.1038/s41598-018-28473-z

Lagaisse R. LifeWatch Belgium: flowCam sampling andlab protocol for imaging microphytoplankton in the Belgian part of the North Sea. protocols.io 2024. https://doi.org/10.17504/protocols.io.6qpvr8e6zlmk/v1

Lanzén A, Jørgensen SL, Huson DH *et al.* CREST–classification resources for environmental sequence tags. *PLoS One* 2012;**7**:e49334. https://doi.org/10.1371/journal.pone.0049334

Lapeyra Martin J, Santi I, Pitta P *et al.* Towards quantitative metabarcoding of eukaryotic plankton: an approach to improve 18S rRNA gene copy number bias. *Metabarcoding and Metagenomics* 2022;**6**:e85794. https://doi.org/10.3897/mbmg.6.85794

Lefebvre A, Guiselin N, Barbet F *et al.* Long-term hydrological and phytoplankton monitoring (19922007) of three potentially eutrophic systems in the eastern English Channel and the Southern Bight of the North Sea. *ICES J Mar Sci* 2011;**68**:2029–43. https://doi.org/10.1093/icesjms/fsr149

Leite BR, Vieira PE, Troncoso JS *et al.* Comparing species detection success between molecular markers in DNA metabarcoding of coastal macroinvertebrates. *Metabarcoding and Metagenomics* 2021;**5**:249–60. https://doi.org/10.3897/mbmg.5.70063

Leray M, Knowlton N, DNA barcoding and metabarcoding of standardized samples reveal patterns of marine benthic diversity. *Proceedings of the National Academy of Sciences*, 2015;**112**:2076–2081. https://doi.org/10.1073/pnas.1424997112

Leray M, Yang JY, Meyer CP *et al.* A new versatile primer set targeting a short fragment of the mitochondrial COI region for metabarcoding metazoan diversity: application for characterizing coral reef fish gut contents. *Frontiers in Zoology* 2013;**10**:1–14. https://doi.org/10.1186/1742-9994-10-34

Lescrauwaet A-K, Pirlet H, Verleye T *et al.*. (Eds.). Compendium voor Kust en Zee 2013: Een geïntegreerd kennisdocument over de socio-economische, ecologische en institutionele aspecten van de kust en zee in Vlaanderen en België. Oostende: Vlaams Instituut voor de Zee (VLIZ), 2013.

Li S, Deng Y, Wang Z *et al.* Exploring the accuracy of amplicon-based internal transcribed spacer markers for a fungal community. *Mol Ecol Resour* 2020;**20**:170–84. https://doi.org/10.1111/1755-0998.13097

Liang Q, Liu Y, Wu S *et al.* Choice of Primer Pairs Affects the eDNA-Based Detection of Eukaryotic Phytoplankton Communities. *Water* 2025;**17**:3173. https://doi.org/10.3390/w17213173

Liu SY, Gibson K, Cui ZM *et al.* Metabarcoding analysis of harmful algal species in Jiaozhou Bay. *Harmful Algae* 2020;**92**:1–12. https://doi.org/10.1016/j.hal.2020.101772

Liu Z, Semmouri I, Li Y *et al.* Earlier onset of phytoplankton bloom in the Southern Bight of the North Sea in response to climate variability. *Mar Environ Res* 2025;**212**:107570. https://doi.org/10.1016/j.marenvres.2025.107570

Liu-Wei W, Van Der Toorn W, Bohn P *et al.* Sequencing accuracy and systematic errors of nanopore direct RNA sequencing. *Bmc Genomics [Electronic Resource]* 2024;**25**:528. https://doi.org/10.1186/s12864-024-10440-w

Meyers SP, Ahearn DG, Gunkel W *et al.* Yeasts from the North Sea. *Mar Biol* 1967;**1**:118–23. https://doi.org/10.1007/BF00386516

Miya M. Environmental DNA Metabarcoding: a novel method for biodiversity monitoring of marine fish communities. *Annual Review of Marine Science*, 2022;**14**:161–85. https://doi.org/10.1146/annurev-marine-041421-082251

Mortelmans J, Aubert A, Reubens J *et al.* Copepods (Crustacea: copepoda) in the Belgian part of the North Sea : trends, dynamics and anomalies. *J Mar Syst* 2021;**220**:103558. https://doi.org/10.1016/j.jmarsys.2021.103558

Mortelmans J, Goossens J, Amadei Martínez L *et al.* LifeWatch observatory data: zooplankton observations in the Belgian part of the North Sea. *Geoscience Data Journal* 2019;**6**:76–84. https://doi.org/10.1002/gdj3

Mortelmans J, Semmouri I, Perneel M *et al.* Temperature-induced copepod depletion and the associated wax of Bellerochea in Belgian coastal waters : implications and shifts in plankton dynamics. *J Sea Res* 2024;**201**:102523. https://doi.org/10.1016/j.seares.2024.102523

Moutinho J, Costa FO, Duarte S. Advancements in DNA Metabarcoding Protocols for Monitoring Zooplankton in Marine and Brackish Environments. *J Mar Sci Eng*, 2024;**12**:2093. https://doi.org/10.3390/jmse12112093

Naito A, Abe Y, Matsuno K *et al.* Surface zooplankton size and taxonomic composition in Bowdoin Fjord, north-western Greenland: a comparison of ZooScan, OPC and microscopic analyses. *Polar Sci* 2019;**19**:120–9. https://doi.org/10.1016/j.polar.2019.01.001

Nohe A, Knockaert C, Goffin A *et al.* Marine phytoplankton community composition data from the Belgian part of the North Sea, 1968–2010. *Sci Data* 2018;**5**:180126 . https://doi.org/10.1038/sdata.2018.126

Novotny A, Rodrigues C, Jacquemot L *et al.*. DNA metabarcoding captures temporal and vertical dynamics of mesozooplankton communities. *ICES Journal of Marine Science* 2025;**82**. https://doi.org/10.1093/icesjms/fsaf007

Oksanen J, Blanchet FG, Kindt R *et al.* Vegan: community Ecology Package. *R Package Version 2.2-0*. 2015 Retrieved August 21, 2020 from http://CRAN.Rproject.org/package=vegan

Oksanen J, Simpson G, Blanchet F *et al. vegan: Community Ecology Package*. R package version 2.8-0. 2026. https://vegandevs.github.io/vegan/ (15 March 2026, date last accessed)

Oxford Nanopore Technologies. *Ligation sequencing amplicons—PCR barcoding (SQK-LSK110 with EXP-PBC096)*. 2023. https://community.nanoporetech.com/docs/prepare/library_prep_protocols/pcr-barcoding-96-amplicons-sqk-lsk110/v/pbac96_9114_v110_revl_10nov2020 (15 March 2026, date last accessed)

Pawlowski J, Audic S, Adl S *et al.* CBOL Protist Working Group: barcoding Eukaryotic Richness beyond the Animal, Plant, and Fungal Kingdoms. *PLoS Biol* 2012;**10**:e1001419. https://doi.org/10.1371/journal.pbio.1001419

Peng X, Amend AS, Baltar F *et al.* Planktonic marine Fungi: a review. *Journal of Geophysical Research: Biogeosciences* 2024;**129**:e2023JG007887. https://doi.org/10.1029/2023jg007887

Perneel M, Lagaisse R, Mortelmans J *et al.* Seasonal metabolic dynamics of microeukaryotic plankton: a year-long metatranscriptomic study in a temperate sea. *mBio* 2024;**15**:e00383–24. https://doi.org/10.1128/mbio.00383-24

Piñol J, Mir G, Gomez-Polo P *et al.* Universal and blocking primer mismatches limit the use of high-throughput DNA sequencing for the quantitative metabarcoding of arthropods. *Mol Ecol Resour* 2014;**15**:819–30. https://doi.org/10.1111/1755-0998.12355

Pomerantz A, Penafiel N, Arteaga A *et al.* Real-time DNA barcoding in a rainforest using nanopore sequencing: opportunities for rapid biodiversity assessments and local capacity building. *GigaScience* 2018;**7**:1–14. https://doi.org/10.1093/gigascience/giy033

Rang FJ, Kloosterman WP, de Ridder J. From squiggle to basepair: computational approaches for improving nanopore sequencing read accuracy. *Genome Biol*, 2018;**19**:90. https://doi.org/10.1186/s13059-018-1462-9

Ratnarajah L, Abu-Alhaija R, Atkinson A *et al.* Monitoring and modelling marine zooplankton in a changing climate. *Nat Commun* 2023;**14**:564. https://doi.org/10.1038/s41467-023-36241-5

Robinson KL, Sponaugle S, Luo JY *et al.* Big or small, patchy all: resolution of marine plankton patch structure at micro- to submesoscales for 36 taxa. *Sci Adv* 2021;**7**:eabk2904. https://doi.org/10.1126/sciadv.abk2904

Rombouts I, Simon N, Aubert A *et al.* Changes in marine phytoplankton diversity: assessment under the Marine Strategy Framework Directive. *Ecol Indic* 2019;**102**:265–77. https://doi.org/10.1016/j.ecolind.2019.02.009

Sahlin K, Lim MCW, Prost S. NGSpeciesID: DNA barcode and amplicon consensus generation from long-read sequencing data. *Ecology and Evolution*, 2021;**11**:1392–8. https://doi.org/10.1002/ece3.7146

Sahlin K, Medvedev P. Error correction enables use of Oxford Nanopore technology for reference-free transcriptome analysis. *Nat Commun*, 2021;**12**:2. https://doi.org/10.1038/s41467-020-20340-8

Santos R, Lee H, Williams A *et al.* Investigating the Performance of Oxford Nanopore Long-Read Sequencing with Respect to Illumina Microarrays and Short-Read Sequencing. *Int J Mol Sci* 2025;**26**:4492. https://doi.org/10.3390/ijms26104492

Sassoubre LM, Yamahara KM, Gardner LD *et al.* Quantification of environmental DNA (eDNA) shedding and decay rates for three marine fish. *Environ Sci Technol* 2016;**50**:10456–64. https://doi.org/10.1021/acs.est.6b03114

Schloss PD. Rarefaction is currently the best approach to control for uneven sequencing effort in amplicon sequence analyses. *mSphere*, 2024;**9**:e0035423. https://doi.org/10.1128/msphere.00354-23

Schoch CL, Ciufo S, Domrachev M *et al.* NCBI Taxonomy: a comprehensive update on curation, resources and tools. *Database* 2020;**2020**:baaa062. https://doi.org/10.1093/database/baaa062

Seah A, Lim MCW, McAloose D *et al.* MinION-based DNA barcoding of preserved and non-invasively collected wildlife samples. *Genes* 2020;**11**:445. https://doi.org/10.3390/genes11040445

Semmouri I, De Schamphelaere K, Mees J *et al.* Evaluating the potential of direct RNA nanopore sequencing: metatranscriptomics highlights possible seasonal differences in a marine pelagic crustacean zooplankton community. *Mar Environ Res* 2020;**153**:104836. https://doi.org/10.1016/j.marenvres.2019.104836

Semmouri I, De Schamphelaere K, Mortelmans J *et al.* Decadal decline of dominant copepod species in the North Sea is associated with ocean warming : importance of marine heatwaves. *Mar Pollut Bull* 2023;**193**:115159. https://doi.org/10.1016/j.marpolbul.2023.115159

Semmouri I, De Schamphelaere K, Willemse S *et al.* Metabarcoding reveals hidden species and improves identification of marine zooplankton communities in the North Sea. *ICES J Mar Sci* 2021;**78**:3411–27. https://doi.org/10.1093/icesjms/fsaa256

Semmouri I, De Schamphelaere KAC, Van Nieuwerburgh F *et al.* Contribution of combined stressors on density and gene expression dynamics of the copepod *Temora longicornis* in the North Sea. *Mol Ecol* 2024b;**34**, e17312. Advance online publication. https://doi.org/10.1111/mec.17312

Semmouri I, Mortelmans J, Roland C *et al.* Decadal trends and dynamics in the abundance and biomass of marine branchiopods in the southern part of the North Sea. *J Mar Syst* 2024a;**245**:103992. Doi: https://doi.org/10.1016/j.jmarsys.2024.103992

Serrana JM, Miyake Y, Gamboa M *et al.* Comparison of DNA metabarcoding and morphological identification for stream macroinvertebrate biodiversity assessment and monitoring. *Ecol Indic* 2019;**101**:963–72. https://doi.org/10.1016/j.ecolind.2019.02.008

Shaffer MR, Andruszkiewicz Allan E, Van Cise AM *et al.* Observation Bias in Metabarcoding. *Mol Ecol Resour* 2025;**25**:e14119. https://doi.org/10.1111/1755-0998.14119

Shannon CE. A mathematical theory of communication. *Bell Syst Tech J* 1948;**27**:379–423. https://doi.org/10.1002/j.1538-7305.1948.tb01338.x

Simpson EH. Measurement of diversity. *Nature*, 1949;**163**:688. https://doi.org/10.1038/163688a0

Song L, Wu J, Du J *et al.* The characteristics and distribution of eukaryotic phytoplankton community in Liaodong Bay, China. *Ocean Sci J* 2019;**54**:183–203. https://doi.org/10.1007/s12601-019-0007-9

Stoeck T, Bass D, Nebel M *et al.* Multiple marker parallel tag environmental DNA sequencing reveals a highly complex eukaryotic community in marine anoxic water. *Mol Ecol* 2010;**19**:21–31. https://doi.org/10.1111/j.1365-294X.2009.04480.x

Srivathsan A, Baloğlu B, Wang W *et al.*. A MinION™-based pipeline for fast and cost-effective DNA barcoding. *Molecular Ecology Resources* 2018;**18**:1035–1049. https://doi.org/10.1111/1755-0998.12890

Suter L, Polanowski AM, Clarke LJ *et al.* Capturing open ocean biodiversity: comparing environmental DNA metabarcoding to the continuous plankton recorder. *Mol Ecol* 2021;**30**:3140–57. https://doi.org/10.1111/mec.15587

Taberlet P, Coissac E, Hajibabaei M *et al.*. Environmental DNA. *Molecular Ecology* 2012;**21**:1789–1793. https://doi.org/10.1111/j.1365-294X.2012.05542.x

Taberlet P, Bonin A, Zinger L *et al. Environmental DNA.* In Oxford University Press eBooks, Oxford University Press, Oxford, UK. 2018. https://doi.org/10.1093/oso/9780198767220.001.0001

Takahashi M, Saccò M, Kestel JH *et al.* Aquatic environmental DNA: a review of the macro-organismal biomonitoring revolution. *Sci Total Environ* 2023;**873**:162322. https://doi.org/10.1016/j.scitotenv.2023.162322

Takasu H, Inomata H, Uchino K *et al.* Spatio-temporal distribution of environmental DNQ derived from Japanese sea nettle jellyfish *Chrysaora pacifica* in Omura Bay, Kyushu, Japan. *Plankton*

*and Benthos Research* 2019;**14**:320–3. https://doi.org/10.3800/pbr.14.320

Thevarajan S, Sun P, Wang P *et al.* Morphological and molecular diversity of phytoplankton in Beibu Gulf, Northern South China Sea. *Ecology and Evolution* 2025;**15:e71207**. https://doi.org/10.1002/ece3.71207

Van Ginderdeuren K, Van Hoey G, Vincx M *et al.* The mesozooplankton community of the Belgian shelf (North Sea). *J Sea Res* 2014;**85**:48–58. https://doi.org/10.1016/j.seares.2013.10.003

Vansteenbrugge L, Ampe B, De Troch M *et al.* On the distribution and population dynamics of the ctenophore *Mnemiopsis leidyi* in the Belgian part of the North Sea and Westerschelde estuary. *Mar Environ Res* 2015b;**110**:33–44. https://doi.org/10.1016/j.marenvres.2015.07.011

Vansteenbrugge L, Van Regenmortel T, De Troch M *et al.* Gelatinous zooplankton in the Belgian part of the North Sea and the adjacent Schelde estuary: spatio-temporal distribution patterns and population dynamics. *J Sea Res* 2015a;**97**:28–39. https://doi.org/10.1016/j.seares.2014.12.008

Vasiljevic N, Lim M, Humble E *et al.* Developmental validation of Oxford Nanopore Technology MinION sequence data and the NGSpeciesID bioinformatic pipeline for forensic genetic species identification. *Forensic Sci Int Genet* 2021;**53**:102493. https://doi.org/10.1016/j.fsigen.2021.102493

Weigand H, Beermann AJ, Čiampor F *et al.* Normalization and microbial differential abundance strategies depend upon data characteristics. *Microbiome* 2017;**5**:27. https://doi.org/10.1186/s40168-017-0237-y

Weigand H, Beermann AJ, Čiampor F *et al.* DNA barcode reference libraries for the monitoring of aquatic biota in Europe: Gap-analysis and recommendations for future work. *Science of The Total Environment* 2019;**678**:499–524. https://doi.org/10.1016/j.scitotenv.2019.04.247

Weirather JL, de Cesare M, Wang Y *et al.* Comprehensive comparison of Pacific Biosciences and Oxford Nanopore Technologies and their applications to transcriptome analysis. *F1000Research* 2017;**6**:100. https://doi.org/10.12688/f1000research.10571.2

Weiss S, Xu ZZ, Peddada S *et al.* Normalization and microbial differential abundance strategies depend upon data characteristics. *Microbiome* 2017;**5**. https://doi.org/10.1186/s40168-017-0237-y

Weydmann-Zwolicka A, Dąbrowska AM, Mioduchowska M *et al.* Comparison of DNA metabarcoding and microscopy in analysing planktonic protists from the European Arctic. *Mar Biodivers* 2024;**54**:44. https://doi.org/10.1007/s12526-024-01436-6

Wick R. Porechop. 2017. https://github.com/rrwick/Porechop (15 March 2026, date last accessed)

Wick RR, Judd LM, Holt KE. Deepbinner: demultiplexing barcoded Oxford Nanopore reads with deep convolutional neural networks. *PLoS Comput Biol*, 2018;**14**:e1006583. https://doi.org/10.1371/journal.pcbi.1006583

Winand R, Bogaerts B, Hoffman S *et al.* Targeting the 16S RRNA gene for bacterial identification in complex mixed samples: comparative evaluation of second (Illumina) and third (Oxford Nanopore Technologies) generation Sequencing Technologies. *Int J Mol Sci* 2020;**21**:298. https://doi.org/10.3390/ijms21010298

WoRMS Editorial Board. *World Register of Marine Species*. VLIZ, Ostend, Belgium. 2020. http://www.marinespecies.org, https://doi.org/10.14284/170 (20 October 2025, date last accessed)

Wyler SA, Bouchez A, Borja A *et al.* DNA barcode reference libraries for the monitoring of aquatic biota in Europe: gap-analysis and recommendations for future work. *Sci Total Environ* 2019;**678**:499–524. https://doi.org/10.1016/j.scitotenv.2019.04.247

Xu X, Yu Z, Cheng F *et al.* Molecular diversity and ecological characteristics of the eukaryotic phytoplankton community in the coastal waters of the Bohai Sea, China. *Harmful Algae* 2016;**61**:13–22. https://doi.org/10.1016/j.hal.2016.11.005

Yang J, Zhang X, Zhang W *et al.* Indigenous species barcode database improves the identification of zooplankton. *PLoS One* 2017;**12**:e0185697. https://doi.org/10.1371/journal.pone.0185697

Zafeiropoulos H, Gargan L, Hintikka S *et al.* The Dark mAtteR iNvestigator (DARN) tool: getting to know the known unknowns in COI amplicon data. *Metabarcoding and Metagenomics* 2021;**5**:163–74. https://doi.org/10.3897/mbmg.5.69657

Zhang GK, Chain FJJ, Abbott CL *et al.* Metabarcoding using multiplexed markers increases species detection in complex zooplankton communities. *Evolutionary Applications* 2018;**11**:1901–14. https://doi.org/10.1111/eva.12694

*Handling editor: Matthew A. Lemay*



**Received:** 11 February 2026. **Revised:** 20 April 2026. **Accepted:** 28 April 2026